POLITECNICO
MILANO 1863

SCUOLA DI INGEGNERIA INDUSTRIALE
E DELL'INFORMAZIONE

A new particle filter application for estimating cutting forces and detecting regenerative instability in milling

Tesi di Laurea Magistrale in
Mechanical Engineering - Ingegneria Meccanica

Author: **Luca Grigis**

Student ID: 963217
Advisor: Prof. Paolo Albertelli
Co-advisors: Luca Bernini
Academic Year: 2021-22

Abstract

The regenerative instability, also known as “chatter”, is a phenomenon that may arise during a milling process and it can lead to failure to achieve the minimum levels of quality and productivity and to the breakage of the tool or of the spindle.Regenerative instability is a process which may arise from the response of the machine to particular cutting conditions, when chip thickness modulation increases up to the point in which the cutting edges detach from the workpiece.

This thesis has the objective to real time estimate tooltip vibrations and cutting forces during stable and unstable milling, and to identify of the possible onset of the aforementioned instability.

The considered system model is based both on the machine dynamics and the cutting process. The study is performed relying on the particle filter, which is a state observer based on Monte Carlo method, which allows dealing with non-linear time delayed differential equations, typical of the analysed phenomenon. The implemented observer was tested with two different type of plant simulations and in real cutting conditions with experimental data.

The estimation results were in general good and reliable and interesting considerations regarding instability and tool detachment came from the chatter indicator behaviour. Possible area of improvements were identified as the reduction of computational cost or the inclusion of cutting parameters as unknown variables.

Keywords: milling process, machine dynamics, cutting forces, chatter instability, state observer, Particle filter

Abstract in lingua italiana

L'instabilità rigenerativa, anche nota come "chatter", è un fenomeno che può svilupparsi durante un processo di taglio e che può portare al mancato raggiungimento degli obiettivi minimi di qualità e produttività e al danneggiamento di utensile e mandrino. L'instabilità rigenerativa è infatti un fenomeno che si origina dalla risposta della macchina a particolari condizioni di lavorazione, quando la modulazione sullo spessore del truciolo cresce fino al punto in cui il tagliente entra ed esce ripetutamente dal materiale.

Questa tesi ha come obiettivo la stima, attraverso un osservatore di stato, delle vibrazioni in punta utensile e delle forze di taglio in condizioni di fresatura stabile e instabile e sull'individuazione della possibile insorgenza della suddetta instabilità. Il sistema considerato si basa sia sulla dinamica della macchina che sul processo di taglio.

Lo studio è stato svolto affidandosi al particle filter, un osservatore basato sul metodo di Monte Carlo che permette di trattare equazioni differenziali non lineari e con ritardo, tipiche del fenomeno preso in esame. L'osservatore è stato valutato con due differenti simulazioni della dinamica della macchina e in vere condizioni di taglio, con dati sperimentali.

In generale, i risultati sono soddisfacenti e il comportamento dell'indicatore di chatter ha portato a considerazioni interessanti riguardo alla formulazione dell'instabilità e del distacco dell'utensile. La riduzione del costo computazionale e l'inclusione dei parametri di taglio come variabili non note sono possibili punti di partenza per futuri miglioramenti.

Parole chiave: fresatura, dinamica della macchina, forze di taglio, instabilità rigenerativa, osservatore di stato, Particle filter

Contents

Introduction

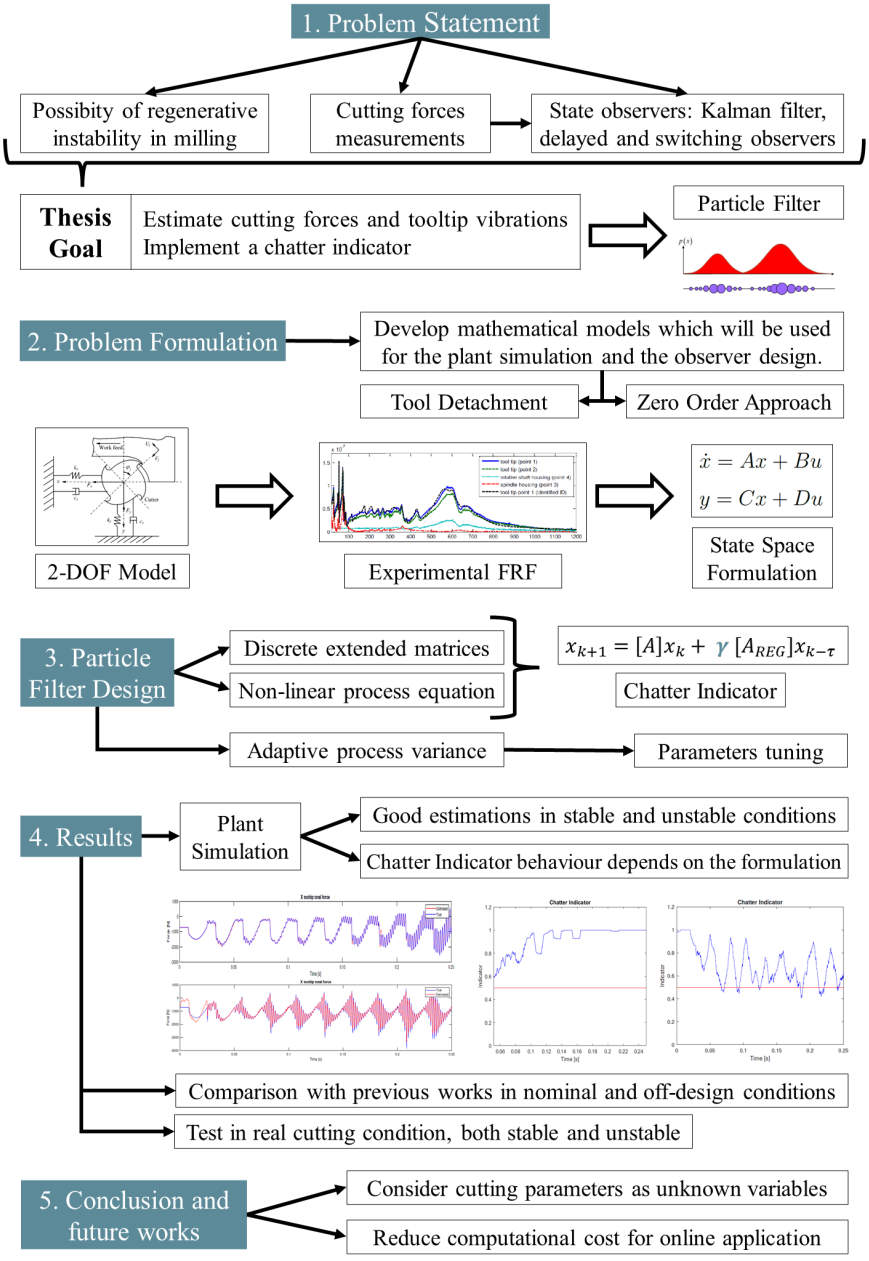

Figure 1: Graphical abstract of the thesis

Figure 1 represents the structure of this thesis. in which a particle filter is designed for the estimation of cutting forces and tooltip vibrations in stable and unstable cutting conditions, a problem already discussed in literature and in which possible area of improvements are defined.

In the last few years, high quality machining became the most crucial aspect in manufacturing, in order to survive in a market in which China, India and other lower-wage countries can offer lower costs. Machine tool builders are focused on designing and building machines which are characterized by high performances (accuracy, reliability, productivity), customizability and high-quality technical support.

As a consequence of the increasing awareness on the climate change, more importance is dedicated to the design of environmentally friendly machines, which has the reduced energy consumption as a primary goal. The industrial sector currently consumes almost one half of the total energy produced (44.1% in Italy in 2020 according to Terna S.p.A., the italian transmission system operator) and improvements in this area could be very impactful. Machine tools will also have another role in the ecological transition. Wind turbines require the production of high-precision blades and bearings, while all sorts of components are machined for the utilisation of hydropower, from simple shafts and bushings to hydro turbine housings, impellers and covers.

Considering the European and Italian situation, the machine tools sector has always been one of the most important. The last available CECIMO report is from 2021. The machine tools income grew up to 22.6 billion euros, a better result than the 20.2 of the 2020 but fare from the 27.4 of the 2019, due to the COVID-19 pandemic. Even in this scenario, Europe was able to keep its share at 34% of the global market. As regards Italy, 2021 income reached 5.7 billion euros, from the 4.7 of the 2020. This is a better result than the European average and its share grew from 23.2 to 25.2% of the CECIMO market.

In order to improve performances in such a difficult market, Industry 4.0 paradigm is a unique opportunity. Machines are becoming smarter and sensorization is becoming cheaper and can be implemented for an increasing number of purposes. In machine tools sector, data as cutting forces, vibrations, surface finish, temperature can be collected to control the production. Thanks to sensors, computers can perform monitoring tasks usually in charge of humans. In fact, data from internal sensors can be an estimator of the cutting quality, but they also show information on the machine or tool status, useful for a better maintenance scheduling which will reduce downtimes and guarantee a performance regularity.

The process for sensor monitoring is divided in the following steps:

- The signal coming from sensors is manipulated in order to obtain a meaningful value about the tool or process state.
- Information is fed to a cognitive decision making system for the correct diagnosis.
- The support system can perform an adaptive or corrective action based on analyzed data or suggest an operation which will be performed by the human operator.

The primary goal of a manufacturing plant is the high productivity and reliability. In order to obtain it, cutting parameters such as axial depth of cut, radial immersion and feed have to be maximized, with the drawback of increasing vibrations and possible instability. Between manufacturing processes, milling is one of the most important and widespread, thanks to its high material removal rate, precision and complexity of geometries which can be obtained. Manufacturing companies strongly require cutting quality and good surface finish, which are influenced by the tool dynamics or, more precisely, by physical variables as tooltip displacement, vibration or deflection and cutting forces.

1 | Problem Statement

1.1. Graphical abstract

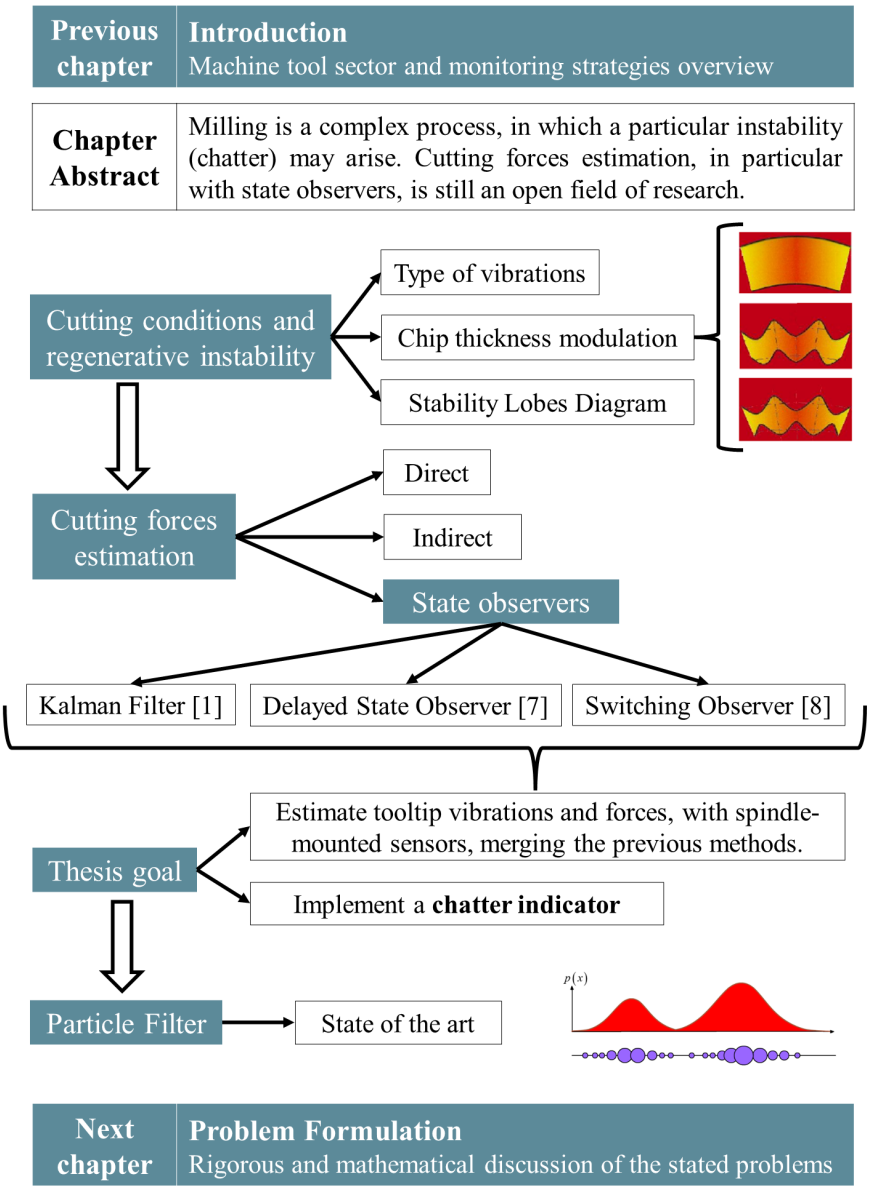

1.2. Cutting conditions and regenerative instability

During a generic cutting process, different types of vibrations can be observed. When their amplitude is increased, they may lead to tool/inserts breakage, faster bearings wearing or unacceptable surface quality. An online estimation of vibrations allows to have a real time information on workpiece quality. Also the growing noise can be a clue for incorrect cutting conditions. In stable conditions, oscillations have a small amplitude and a random pattern. Higher amplitudes and the presence of a predominant frequency component are synonymous of unstable conditions (Figure 1.1).

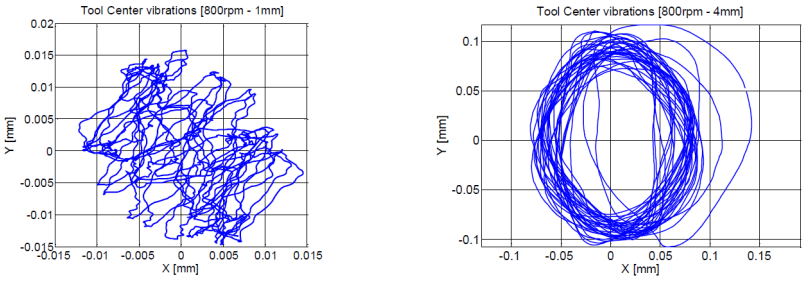

(a) Stable vibrations (b) Unstable vibrations

Figure 1.1: Different vibrations in stable and unstable conditions

It is possible to identify three main types of vibration, each of them being responsible of a different chip shape as shown in Figure 1.2:

- Free vibrations, which are due to a perturbation from from the equilibrium state. They are damped over time with an oscillatory motion.
- Forced vibration, as a result of a continuous perturbation and coherently with the frequency response function.
- Self-excited vibrations, which occur when the structure is not able to damp the energy introduced in the system from the interaction between workpiece and tool.

Self-excited vibrations are unstable vibrations originated from friction, mode coupling or regenerative phenomena. In this thesis, "chatter" will identify the regenerative instability occurring when the oscillation of the tooltip in one pass of the tool leaves a waved mark on the machined surface, which will be regenerated by the following tooth. This oscillatory motion generates a modulation of chip thickness and cutting forces, which leads to an indefinite increase of the amplitude of vibrations. Actually, it can be observed that after

a certain value of amplitude, the loss-of-contact between tool and workpiece occurs and the amplitude will not further increase.

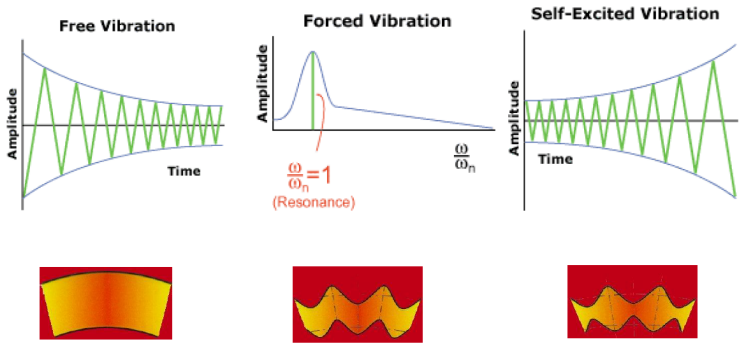

Figure 1.2: Effects of different vibrations on the chip shape.

Depth of cut and spindle speed are the two parameters which can be tuned in order to avoid chatter. The most important contribution in this area was provided in 1995 by Altintas and Budak [3]. Starting from:

- Transfer functions of the structure at the cutter-workpiece contact zone
- Static cutting force coefficients
- Radial immersion and number of teeth on the cutter
- Time varying dynamic cutting force coefficients, approximated by their Fourier series components arrested at zero order (Zeroth Order Approach, ZOA)

it is possible to analitically predict the stability of the cutting process. Stability Lobes Diagrams (SLD) are obtained from the resolution of the dynamic equilibrium equation with regenerative effect. They show on the abscissas axis the spindle speed and on the ordinates axis the axial depth of cut. A selection of this two parameters so that the point relies below the line can assure stable conditions.

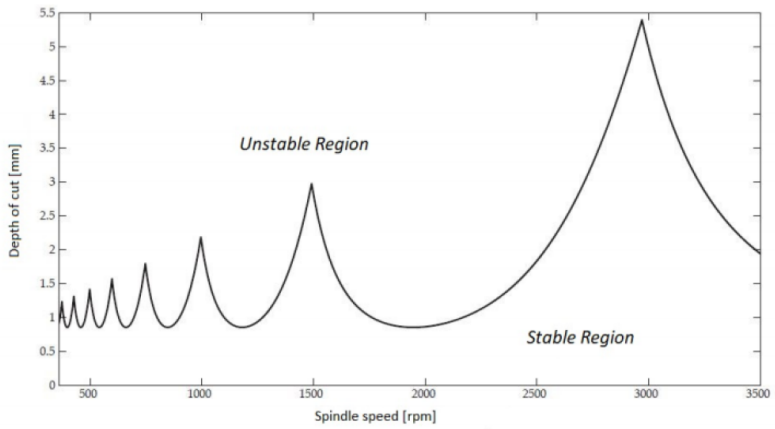

Figure 1.3: Stability Lobes Diagrams (SLD).

1.3. Cutting forces and vibrations estimation

During a milling process, the measurement of cutting forces is a possible monitoring and control strategy. As anticipated in the introduction, cutting forces can provide information about cutting conditions and tool engagement, surface quality, tool wear and others. There are two ways to measure cutting forces:

- Direct measurements
- Indirect measurements.

Talking about direct measurements, piezoelectric dynamometers are the most common sensors. Fixed dynamometers are mounted between the work table and the workpiece (Figure 1.4) and the force is transmitted from the workpiece to the sensors. Alternatively, rotating piezoelectric dynamometers are mounted between the spindle and the tool, and they are also able to measure torque, in addition to three directions forces. These devices are not widespread in the industrial environment, because of their limited size, setting difficulties and high costs and because they can reduce the machine stiffness. Piezoelectric measurements will also include the workpiece inertia, if the workpiece is moved during the machining operation.

Indirect measurements rely on a model explaining the relationship between the force magnitude and the instrument reading. Altintas and Park show a possible setup [4]: Spindle Integrated Force Sensors (SIFS) are placed into the stationary spindle housing (Figure 1.5) and the structural dynamic model between the cutting forces at the tool tip and the measured forces is identified. This approach allows significant advantages:

- Machine working space and cutting capabilities are not modified

- Workpiece size is not reduced
- Sensors are not directly exposed to chip or coolant.

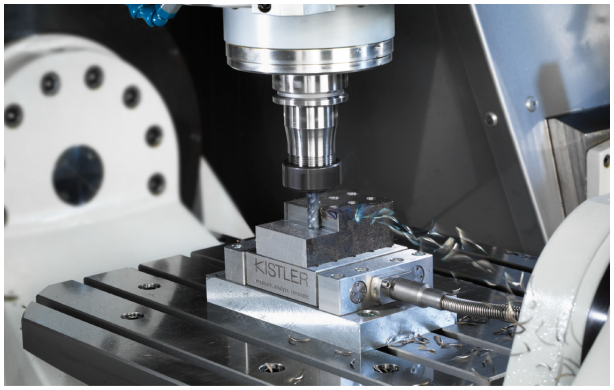

Figure 1.4: Fixed dynamometer (courtesy of Kistler)

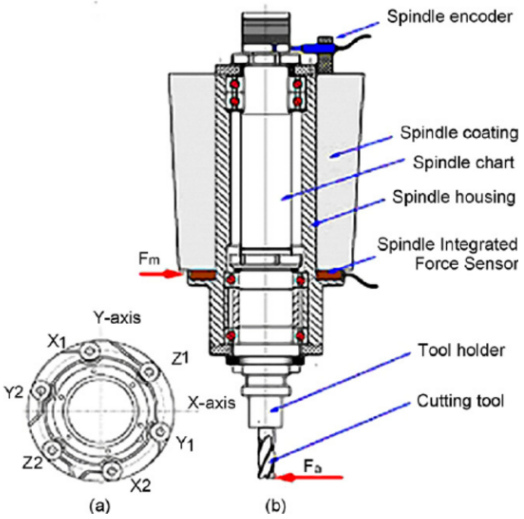

Figure 1.5: SIFS configuration

Another possible indirect method relies on current drawn measurement, since the motor load is proportional to the current. Unfortunately, this load does not include only the cutting force, but also the effect of path and motion laws, control actions, dynamics of the drive chain and friction. A reliable dynamic model describing the transmission of forces from the tooltip to the drive can be difficult to be implemented.

A powerful method, which can be considered as an indirect force measurement, is the implementation of a state observer. State observers are systems able to estimate the internal states of the real systems from the measurements of inputs and outputs. In

addition to the same advantages of indirect measurements, they offer the possibility to use simple spindle-mounted sensors, such as accelerometers and inductive displacement sensors, so a modified or retrofitted machine is not needed. A deeper discussion on state observers implementation will be provided in the next chapters.

1.4. State observers for cutting forces estimation

In this thesis, state observers based on the Kalman filter will be considered the State of the Art [12]. Equation (1.1) shows the continuous time system in state-space form, in which x, u and y are respectively state, input and measurement vectors, while A, B, C and D are systems matrices.

$$\dot{x} = Ax + Bu \tag{1.1a}$$

$$y = Cx + Du \tag{1.1b}$$

The state observer is designed introducing a corrective term on the measurement residual.

$$\dot{\hat{x}} = A\hat{x} + Bu + L(y - \hat{y}) \tag{1.2a}$$

$$\hat{y} = C\hat{x} + Du \tag{1.2b}$$

L is the gain matrix, while $\hat{x}$ and $\hat{y}$ are the estimated states and measurements, respectively. The state estimation error can be defined as $e = x - \hat{x}$ and its dynamic equation can be rewritten as:

$$\dot{e} = (A - LC)e \tag{1.3}$$

L will be set in order to stabilize the term $(A - LC)$. It can be seen as the gain of the residual: it will be higher if the measurement is more reliable than the model and viceversa. Kalman filter provides a state estimation for linear systems under the hypothesys of Gaussian noise. Its estimation is optimal, since the state covariance matrix is minimized.

It is possible to find several works in literature about the use of the Kalman filter in cutting force estimation in machining. For instance, piezo-electric load sensors mounted in the spindle housing were used by Altintas and Park in the already cited work [4], and their measurements were processed by a Kalman filter in order to compensate the effects of structural flexibility on the force measurement. Albrecht et al. [2] developed an indirect method for measuring the cutting forces, based on the spindle shaft displacements measurements performed with capacitance sensors. Albertelli et al. [1] developed an estimator according to the Kalman Filter approach, which relies on both a machine dynamic model and on indirect measurements coming from multiple sensors placed in the machine. The

machine dynamic model was obtained through an experimental modal analysis session, which will be investigated in the next chapters.

Starting from Equation (1.1), the system is modified in order to consider also the input (in this case, the cutting forces) as a state variable.

$$\left\{ \begin{array}{c} \dot{x} \\ \dot{F} \end{array} \right\} = \left[\begin{array}{cc} [A] & [B] \\ [0] & [0] \end{array} \right] \left\{ \begin{array}{c} x \\ F \end{array} \right\} \tag{1.4a}$$

$$\left\{ y \right\} = \left[\begin{array}{cc} [C] & [D] \end{array} \right] \left\{ \begin{array}{c} x \\ F \end{array} \right\} \tag{1.4b}$$

The vector y contains measurements coming from sensors placed on the spindle: spindle shaft-housing relative displacements and housing accelerations, in both directions. Measurement and process noises were of course considered for the calculation of the optimal gain. The model was validated by experimental sessions and good results were achieved in the estimation of tooltip vibrations and cutting forces in stable conditions.

Starting from Albertelli's paper, Marzatico [9] developed a state observer based on the Riccati Equation approach. It allowed a design methodology of state observers for state delayed system described by Delayed Differential Equations.

$$\dot{x(t)} = Ax(t) + A_r x(t-\tau) + BF(t) \tag{1.5}$$

Equation (1.5) includes the term $A_r x(t-\tau)$, which represents the regenerative contribution provided by subsequential passes (with delay τ) of the teeth. The Riccati Equation approach allows the calculation of the gain matrix L including both nominal and regenerative matrices. The delayed observer performed better than the Kalman filter in unstable conditions, thanks to the introduction of A_r, calculated with the Zero-Order approach and including several cutting parameters.

The last theoretical contribution in this field of research was provided by Torricella [11], who included the detachment phenomenon in the state observer formulation, which was not considered in Marzatico's work. It is known that when a high amplitude of vibration is obtained, the tool can loose contact with the material, so the oscillation does not grow indefinitely. The model relies on the assumption that, when the detachment verifies, the system will not undergo the action of the cutting forces. Keeping the extended formulation with forces as state variables, the switching observer will consider Equation (1.6a) when

the tool is engaged and Equation (1.6b) when the detachment is occurring.

$$\begin{Bmatrix} \dot{x} \\ \dot{F} \end{Bmatrix} = \begin{bmatrix} [A] & [B] \\ [0] & [0] \end{bmatrix} \begin{Bmatrix} x \\ F \end{Bmatrix} \tag{1.6a}$$

$$\begin{Bmatrix} \dot{x} \\ \dot{F} \end{Bmatrix} = \begin{bmatrix} [A] & [0] \\ [0] & [0] \end{bmatrix} \begin{Bmatrix} x \\ F \end{Bmatrix} \tag{1.6b}$$

Torricella's work proposes a simplified version of hybrid observers, but a real implementation was never performed.

1.5. Purpose of the thesis

The goal of this thesis is the development of a state observer based on a particle filter for the estimation of cutting forces and tooltip vibrations, in stable and unstable cutting conditions. Milling is a complex process, difficult to be fully described with the simple state-space formulation. As anticipated, the particle filter can both manage delayed and non-linear systems, which previous works were not able to merge in the same observer: these characteristics will be exploited to merge delayed and switching observers. An important innovation will be the implementation of a chatter indicator. It is a state variable considered in the state equation, which will change its value if the instability condition occurs. Thanks to this formulation, it will be possible to consider the regenerative contribution only when needed and to understand if higher forces and vibrations are a consequence of different engagement conditions or of the rising instability. This update is expected to bring an important improvement of the tracking performances of the observer.

In the first part, the system dynamics will be simulated with the Zero-Order Approach. Then, it will be simulated considering the modulation of the chip thickness and the detachment phenomenon. The implemented observer and its performances will be tested with both models, in stable and unstable conditions. The observer will also be tested in non-ideal conditions, with slightly wrong cutting parameters, in order to validate the robustness of the algorithm and compare its performances with previous models.

The last section will be dedicated to the test of the implemented observer in real cutting conditions, both stable and unstable, with experimental data coming from the MUSP laboratory.

1.6. Particle filters for estimations problem, state of the art

Karlsson [7] provided a full review on particle filter algorithms, with a clear explanation on their implementation. In estimation problems the task is to estimate unknown quantities from noisy observations. For linear systems with a Gaussian noise assumption it is possible to derive a finite dimensional solution for the estimate (Kalman Filter). For many practical problems, linear models or the assumption of Gaussian noise, are not plausible. Particle filters, or sequential Monte Carlo methods, provide general solutions to many problems, where linearizations and Gaussian approximations are intractable or would yield too low performances.

Consider the following discrete-time state space description.

$$x_{k+1} = f(x_k, w_k) \tag{1.7a}$$

$$y_k = h(x_k, e_k) \tag{1.7b}$$

The state vector x_k represents the unknown states or parameters at discrete-time index k. The observation y_k is often a nonlinear mapping of the current state. Inaccuracies in the system model and in the measurement relation are described by the stochastic processes w_t and e_t.

The non linear prediction density $p(x_{k+1}|y_k)$ and the filtering density $p(x_k|y_k)$ for the Bayesian inference are given below.

$$p(x_{k+1}|Y_k) = \int p(x_{k+1}|x_k)p(x_k|Y_k)dx_k \tag{1.8a}$$

$$p(x_k|Y_k) = p(Y_k|x_k)p(x_k|Y_{k-1}) \tag{1.8b}$$

The particle filter approximates the probability density $p(x_k|y_k)$ by a large set of N particles $\{x_k{}^{(i)}\}_{i=1}^{N}$, where each particle has an assigned relative weight $\gamma_k^{(i)}$. The weight of each particle reflects the value of the density in that region of the state space. The main idea of the particle filter is to approximate $p(x_k|Y_{k-1})$ with samples, according to equation (1.9), where δ is the Kronecker delta.

$$p(x_k|Y_{k-1}) \sim \frac{1}{N}\sum_{i=1}^{N}\delta(x_k - x_k^{(i)}) \tag{1.9}$$

A basic implementation of the particle filter is shown in the following algorithm.

Algorithm 1.1 Particle Filter

1: Set $t = 0$, generate N samples $\{x_k{}^{(i-)}\}_{i=1}^{N}$ (anterior distribution) from the initial distribution $p_{x_0}(x_0)$.
2: Compute the residual weigths $\gamma_k^{(i)} = p(y_k|x_k^{(i-)})$.
3: Generate the posterior distribution $\{x_k{}^{(i+)}\}_{i=1}^{N}$ by resampling N times from $\{x_k{}^{(i-)}\}_{i=1}^{N}$.
4: Predict new particles $x_{k+1}^{(i-)} = f(x_k^{(i+)}, w)$.
5: Increase t and continue from step 2.

Figure 1.6 offers a graphical representation of one possible resampling strategy. The basic principle is that particles with small weights are likely to be discarded and particles with large weights are copied, so that the number of copies reflects the probability of the particle. This can be done by iterating over the ordered uniform samples $u(j) = \mathcal{U}(0,1)$ with $j = 1, ..., N$ and comparing the cumulative sum of importance weights up to the current index. If the residual weight $\gamma_k^{(i)}$ is large enough to includes two samples of the ordered uniform variables, the corresponding particle $x_k^{(i-)}$ is duplicated and replaces a bad particle. Another approach is to utilize deterministic resampling, calculating the number of particles to be copied by using $N^{(i)} = N_\gamma{}^{(i)}$, which could be somewhat faster. In alternative, an efficient sort function can be used. In [5], four different resampling schemes are compared with respect to their computational complexity and performance.

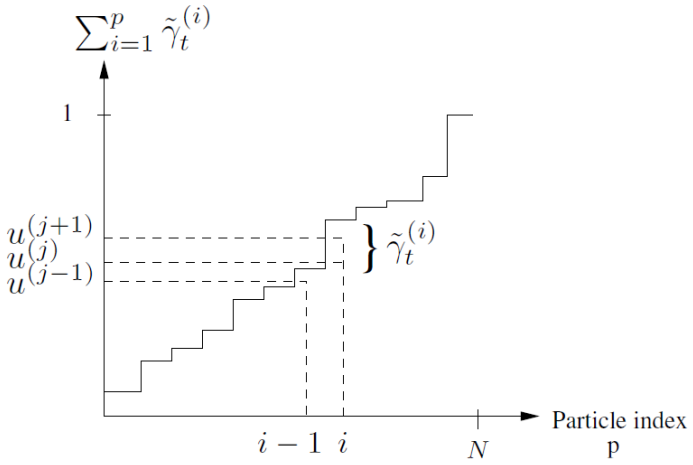

Figure 1.6: Graphical interpretation of the resampling strategy

2 | Problem formulation

2.1. Graphical abstract

Previous chapter	**Problem statement** Possible problems, state of the art and previous works review.
Chapter Abstract	The mathematical description of the plant is provided. It will be used both for simulation and for the state observer design. The FRFs are used to develop a state space system, with a particular focus on the input vector formulation.

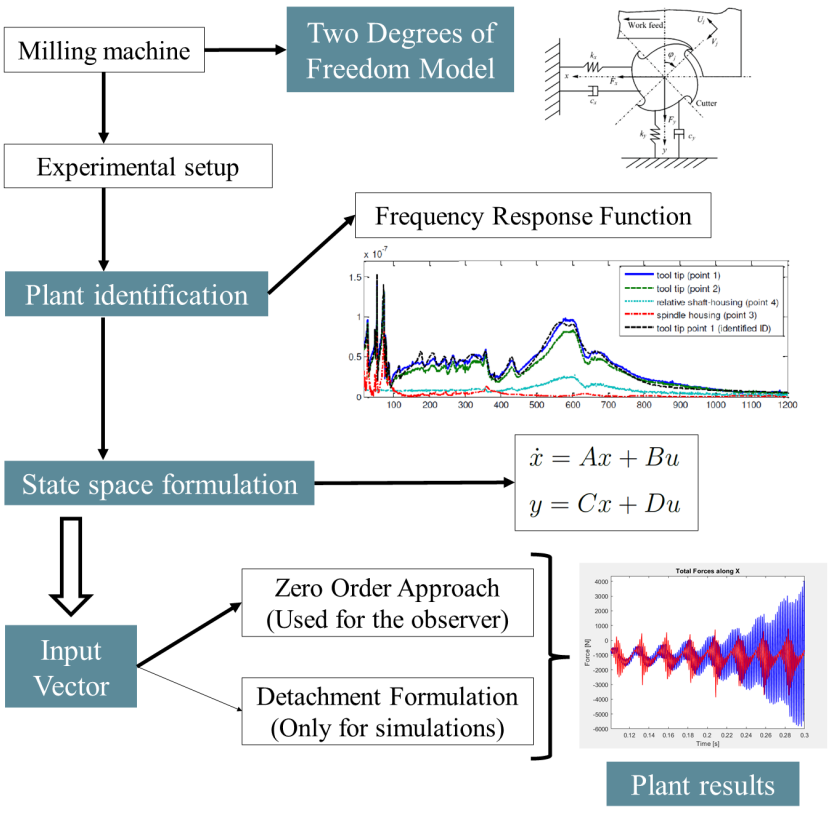

Next chapter	**Particle filter design** Accurate description of the implemented algorithm

2.2. Two degrees of freedom model

A milling system can be reduced to 2-DOF vibration system in the two orthogonal directions [8] as shown in Figure 2.1.

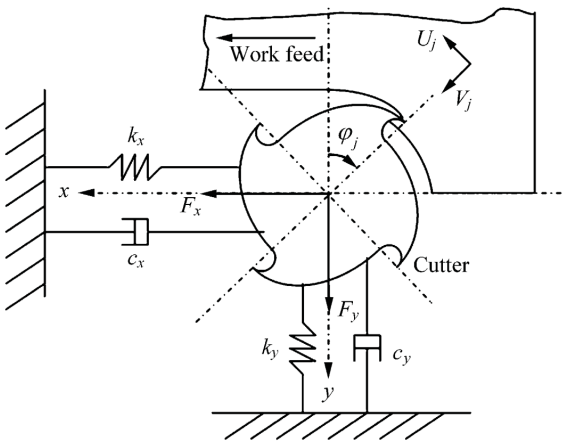

Figure 2.1: Dynamic model of milling system

The dynamics of the milling system can be described by the differential equations:

$$m_x\ddot{x} + c_x\dot{x} + k_x x = F_x(t) \tag{2.1a}$$

$$m_y\ddot{y} + c_y\dot{y} + k_y y = F_y(t) \tag{2.1b}$$

where m, c and k are mass, damping coefficient and stiffness, respectively. They can be rearranged as:

$$\begin{Bmatrix} \ddot{x} \\ \ddot{y} \end{Bmatrix} + \begin{bmatrix} 2\xi\omega_x & 0 \\ 0 & 2\xi\omega_y \end{bmatrix} \begin{Bmatrix} \dot{x} \\ \dot{y} \end{Bmatrix} + \begin{bmatrix} \omega_x^2 & 0 \\ 0 & \omega_y^2 \end{bmatrix} \begin{Bmatrix} x \\ y \end{Bmatrix} = \begin{Bmatrix} F_x \\ F_y \end{Bmatrix} \tag{2.2}$$

in order to highlight the fact that the system is uncoupled. ξ is the damping ratio and ω is the natural frequency of the considered direction. The total force acting on both axes can be expressed as the projection of the sum of the contribution of each active tooth.

2.3. Plant identification

The modal identification carried out in [1] has the aim of identifying the vibration modes of the considered milling machine. The tool parameters are:

- number of teeth, $N = 4$;

- tool diameter, $D = 80mm$.

The sensors configuration used during the modal identification procedure is shown in Figure 2.2.

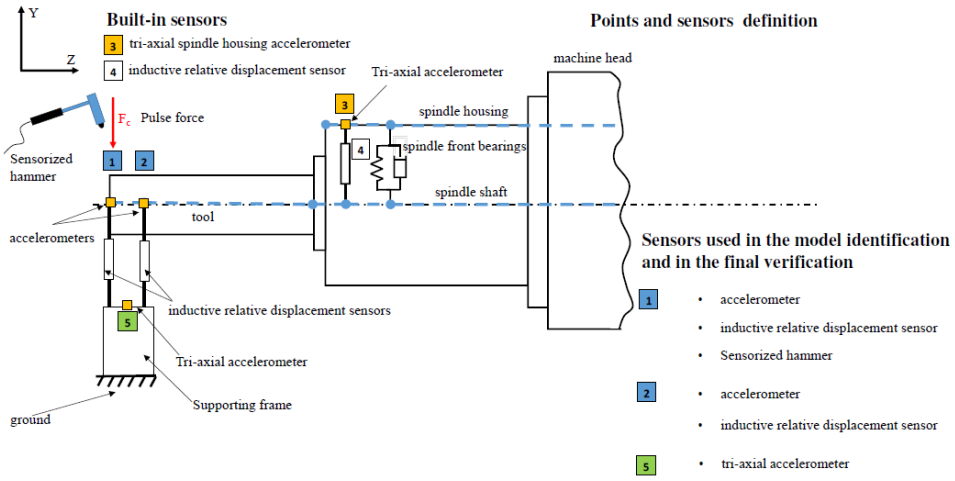

Figure 2.2: Sensors for model identification

The analysis is performed with a sensorized hammer, able to excite the structure in a target range of frequencies. A high number of vibration modes ($n = 32$ total, 21 along x and 11 along y, Figure 2.3) is identified from the frequency response function (Figure 2.4) of the instruments, which are inductive relative displacements sensors on the tooltip, tri-axial spindle housing accelerometers and inductive relative displacements sensors on the spindle housing, in order to have a reliable model also at high frequencies, where chatter occurs.

	X direction					Y direction		
Mode	$\omega_j/(2\pi)$ [Hz]	ζ_j	Mode	$\omega_j/(2\pi)$ [Hz]	ζ_j	Mode	$\omega_j/(2\pi)$ [Hz]	ζ_j
1	28.0	0.069	12	288.0	0.033	1	64.2	0.096
2	48.8	0.006	13	329.7	0.097	2	84.7	0.142
3	54.2	0.008	14	357.8	0.019	3	138.0	0.131
4	72.6	0.027	15	381.9	0.003	4	211.1	0.129
5	78.5	0.013	16	433.0	0.025	5	247.6	0.030
6	86.5	0.035	17	568.2	0.088	6	265.6	0.012
7	116.2	0.015	18	600.8	0.018	7	299.1	0.100
8	179.7	0.025	19	662.9	0.028	8	430.6	0.088
9	214.9	0.054	20	769.6	0.087	9	571.4	0.077

Figure 2.3: Identified eigenmodes for X and Y directions

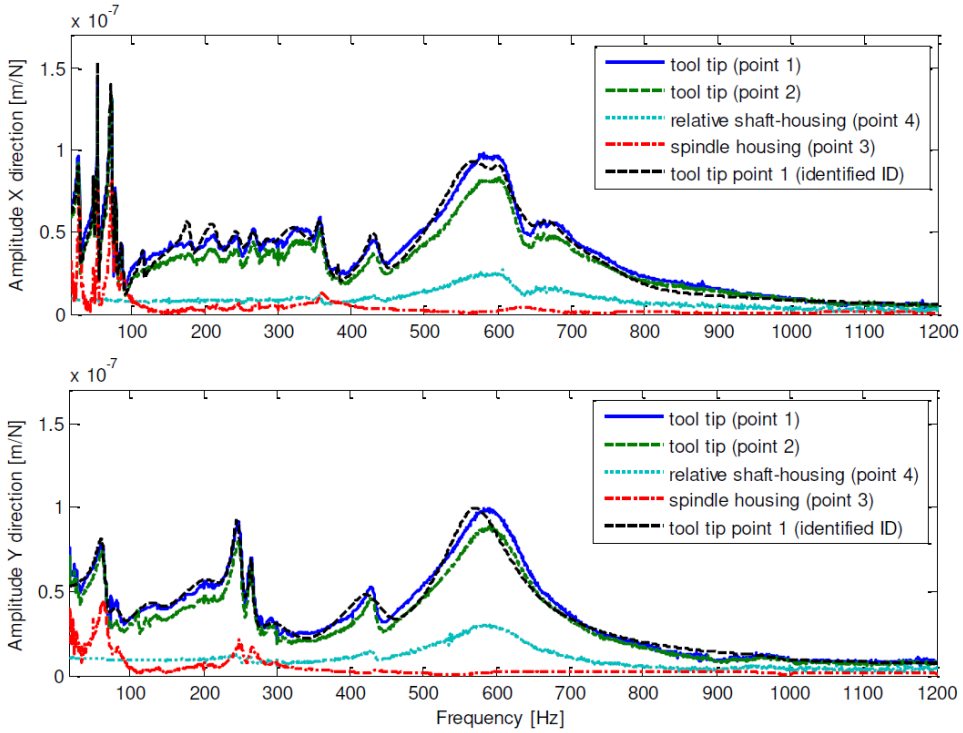

Figure 2.4: Experimental FRFs (amplitudes) along X-Y directions

The system dynamics is described by the equation:

$$\left[\ \mathbf{M}s^2 + \mathbf{R}s + \mathbf{K}\ \right] p(s) = F(s) \tag{2.3a}$$

$$y(s) = \mathbf{g}p(s) \tag{2.3b}$$

where $\mathbf{M}$, $\mathbf{R}$ and $\mathbf{K}$ are respectively mass, damping and stiffness matrices, $F(s)$ is the input, $p(s)$ is the model coordinates vector and $\mathbf{g}$ is the output matrix. It is possible to use the eigenvector matrix $\mathbf{\Phi}$, in order to decouple the equations and get the modal coordinates of the system $q(s)$.

$$p(s) = \mathbf{\Phi}q(s) \tag{2.4}$$

Substituting Equation (2.4) in (2.3), it is possible to obtain the uncoupled system in modal coordinates.

$$\left[\ \mathbf{I}s^2 + \mathbf{\Gamma}s + \mathbf{\Omega^2}\ \right] q(s) = \mathbf{\Phi}^T F(s) \tag{2.5a}$$

$$y(s) = \mathbf{g\Phi}q(s) = \mathbf{C}q(s) \tag{2.5b}$$

I is the identity matrix, while $\mathbf{\Gamma}$ and $\mathbf{\Omega^2}$ can be expressed as:

$$\mathbf{\Gamma} = \begin{bmatrix} 2\xi_1\omega_1 & 0 & 0 & 0 & 0 \\ 0 & 0 & 0 & 0 & 0 \\ 0 & 0 & 2\xi_i\omega_i & 0 & 0 \\ 0 & 0 & 0 & 0 & 0 \\ 0 & 0 & 0 & 0 & 2\xi_n\omega_n \end{bmatrix} \qquad \mathbf{\Omega^2} = \begin{bmatrix} \omega_1^2 & 0 & 0 & 0 & 0 \\ 0 & 0 & 0 & 0 & 0 \\ 0 & 0 & \omega_i^2 & 0 & 0 \\ 0 & 0 & 0 & 0 & 0 \\ 0 & 0 & 0 & 0 & \omega_n^2 \end{bmatrix} \tag{2.6}$$

2.4. State space formulation

In order to design the observer, the system is rearranged in order to obtain the state-space formulation, already presented in Equation (1.1).

$$\dot{x} = Ax + Bu \tag{2.7a}$$

$$y = Cx + Du \tag{2.7b}$$

The state vector x contains the modal coordinates $\{\dot{q}_1 \quad q_1 \quad ... \quad \dot{q}_i \quad q_i \quad ... \quad \dot{q}_n \quad q_n\}$, u is the force input vector, while y is the $4x1$ measurements vector containing displacements and accelerations coming from spindle mounted sensors. From the manipolation of Equation (2.5), it is possible to obtain the state space matrices.

$$A = \begin{bmatrix} 0 & 1 & 0 & 0 & 0 & 0 \\ -\omega_1^2 & -2\xi_1\omega_1 & 0 & 0 & 0 & 0 \\ 0 & 0 & 0 & 1 & 0 & 0 \\ 0 & 0 & -\omega_i^2 & -2\xi_i\omega_i & 0 & 0 \\ 0 & 0 & 0 & 0 & 0 & 1 \\ 0 & 0 & 0 & 0 & -\omega_n^2 & -2\xi_n\omega_n \end{bmatrix} \qquad B = \begin{bmatrix} 0 & 0 \\ \Phi_{1,1}^T & \Phi_{1,2}^T \\ 0 & 0 \\ \Phi_{i,1}^T & \Phi_{i,2}^T \\ 0 & 0 \\ \Phi_{n,1}^T & \Phi_{n,2}^T \end{bmatrix} \tag{2.8}$$

$$C = \begin{bmatrix} g\Phi_{1,1} & 0 & g\Phi_{1,i} & 0 & g\Phi_{1,n} & 0 \\ g\Phi_{2,1} & 0 & g\Phi_{2,i} & 0 & g\Phi_{2,n} & 0 \\ g\Phi_{3,1} & 0 & g\Phi_{3,i} & 0 & g\Phi_{3,n} & 0 \\ g\Phi_{4,1} & 0 & g\Phi_{4,i} & 0 & g\Phi_{4,n} & 0 \end{bmatrix} \qquad D = [0]$$

2.5. Input vector and regenerative contribution

The input vector consists of the cutting forces acting on the system. As previously stated, the total force along x and y is the projection of the sum of the contribution of each active tooth, whose transmitted force is proportional to the chip thickness. Chip thickness h is the sum of a nominal component, due to the feed rate of the tool, and a dynamic one, coming from tool vibrations.

$$h(\varphi_j) = [s_t \sin\varphi_j + (v_{j-1} - v_j)]g(\varphi_j) \tag{2.9}$$

s_t is the standard feed, (v_{j-1}, v_j) are the tooltip displacements of the previous and actual tooth. φ_j is the angular position of each tooth, expressed as $\varphi_j(t) = (\frac{2\pi\Omega}{60})t + \frac{2\pi}{N}j$, where Ω is the angular speed [rpm] of the spindle and N is the number of teeth. The function $g(\varphi_j)$ is a unitary window function that limits the computation of the chip thickness only when the tooth is engaged in the workpiece, expressed as follows.

$$\begin{cases} g(\varphi_j) = 1 & \text{if} \quad \varphi_{in} \leq \varphi_j \leq \varphi_{out} \\ g(\varphi_j) = 0 & \text{else} \end{cases} \tag{2.10}$$

Considering $\Delta x = x_{j-1} - x_j$ and $\Delta y = y_{j-1} - y_j$, as the differences in tooltip displacements between previous and current tooth along X and Y directions, it is possible to finally write the modulated chip thickness as:

$$h(\varphi_j) = [(s_t + \Delta x)\sin\varphi_j + \Delta y \cos\varphi_j]g(\varphi_j) \tag{2.11}$$

The tangential and radial forces for each tool can be expressed as:

$$F_{t,j} = K_t a h(\varphi_j) \qquad F_{r,j} = K_r F_{t,j} \tag{2.12}$$

where K_t and K_r are costant cutting coefficients and a is the axial depth of cut. The total forces along both directions are:

$$F_x = \sum_j -F_{t,j}\cos\varphi_j - F_{r,j}\sin\varphi_j \tag{2.13a}$$

$$F_y = \sum_j F_{t,j}\sin\varphi_j - F_{r,j}\cos\varphi_j \tag{2.13b}$$

Once that total forces are obtained, two different methods are now proposed in order to highlight and exploit the difference between nominal and regenerative contribution.

2.5.1. Zero Order Approach

This formulation is the one proposed by Altintas [3] and used more recently by Marzatico in the development of his delayed observer [9]. It is also the formulation used as the starting point of the particle filter. The general idea is to work on the regenerative contribution of the forces in a matrix form, in order to write the system in a time-delay form:

$$\dot{x(t)} = Ax(t) + A_r x(t-\tau) + BF_{nom}(t) \tag{2.14}$$

F in this case is comprehensive of the lone nominal contribution. The expression of the regenerative force component, indicated as F_{reg} is the following:

$$\begin{Bmatrix} F_{x,reg} \\ F_{y,reg} \end{Bmatrix} = \frac{1}{2} a K_t \begin{bmatrix} a_{xx} & a_{xy} \\ a_{yx} & a_{yy} \end{bmatrix} \begin{Bmatrix} \Delta x \\ \Delta y \end{Bmatrix} \tag{2.15}$$

where matrix entries are time varying directional dynamic milling force coefficients. In a more compact form:

$$\{F_r(t)\} = \frac{1}{2} a K_t [A(t)] \{\Delta(t)\} \tag{2.16}$$

Substituting (2.16) in (2.2):

$$\begin{Bmatrix} \ddot{x}(t) \\ \ddot{y}(t) \end{Bmatrix} + \begin{bmatrix} 2\xi\omega_x & 0 \\ 0 & 2\xi\omega_y \end{bmatrix} \begin{Bmatrix} \dot{x}(t) \\ \dot{y}(t) \end{Bmatrix} + \begin{bmatrix} \omega_x^2 & 0 \\ 0 & \omega_y^2 \end{bmatrix} \begin{Bmatrix} x(t) \\ y(t) \end{Bmatrix} = \begin{bmatrix} F_{x,nom} \\ F_{y,nom} \end{bmatrix} + \frac{1}{2} a K_t [A(t)] \begin{Bmatrix} x(t) - x(t-\tau) \\ y(t) - y(t-\tau) \end{Bmatrix} \tag{2.17}$$

The system is now described by delayed differential equations with time-varying coefficients. The next step is the approximation of the time-varying matrix $[A(t)]$ with a matrix of constant coefficients. It can be observed that the entries of $[A(t)]$ are periodic with freqency $\omega = N\Omega$. The Fourier decomposition allows to consider only the first r harmonics. The Zero order method consists of negletting all the harmonic components ($r = 0$) and considering only the average contribution.

$$[A_r] = \frac{1}{T} \int_0^T [A(t)] e^{-ir\omega_t t} dt \tag{2.18}$$

$$[A_0] = \frac{1}{T} \int_0^T [A(t)] dt \tag{2.19}$$

Equation (2.19) can be written as a function of the tooth angle.

$$[A_0] = \frac{N}{2\pi}\int_{\varphi_{in}}^{\varphi_{out}} [A(\varphi)]d\varphi = \frac{N}{2\pi}\begin{bmatrix} \alpha_{xx} & \alpha_{xy} \\ \alpha_{yx} & \alpha_{yy} \end{bmatrix} \tag{2.20}$$

Equation (2.19) can now be written with a matrix of constant entries:

$$\{F_r(t)\} = \frac{1}{2}aK_t[A_0]\{\Delta(t)\} \tag{2.21}$$

The state-space system is fully described in the required time-delay form, as shown in Equation (2.14)

2.5.2. Tool detachment formulation

Another possible formulation of the plant behaviour is the one proposed by Torricella [11]. The starting point is Equation (2.13), the same of the Zero Order approach, while the difference is the target formulation. It is not required to obtain a time-delay system but a common state space formulation, in which the input vector contains both the nominal and the regenerative contribution of the force.

$$\dot{x(t)} = Ax(t) + BF_{tot}(t) \tag{2.22}$$

It is possible to affirm that in this case the dynamic oscillation of the tooltip never "leaves" the input vector. The complete expression of the chip thickness is:

$$h(\varphi_j) = \left(st\sin\varphi_j + \begin{bmatrix} \sin\varphi_j & \cos\varphi_j \end{bmatrix} \begin{bmatrix} x(t) - x(t-\tau) \\ y(t) - y(t-\tau) \end{bmatrix} \right) g(\varphi_j) \tag{2.23}$$

The function $g(\varphi_j)$ is the same unitary window function that limits the computation of the chip thickness only when the tooth is engaged in the workpiece, shown in Equation (2.10). Another condition is required in order to enforce the detachment of the tool from the workpiece:

$$\begin{cases} h(\varphi_j) = h(\varphi_j) & \text{if} \quad h(\varphi_j) > 0 \\ h(\varphi_j) = 0 & \text{if} \quad h(\varphi_j) \leq 0 \end{cases} \tag{2.24}$$

Except from the Zero Order method, the last equation is the main difference with the Marzatico's formulation, in which the chip thickness can grow indefinitely, also in the negative half-plane. Once chip thickness h is fully described, it is possible to substitute it in Equations (2.12) and (2.13) and obtain the complete input vector $F_{tot}(t)$.

2.6. Plant results

The plant was simulated in a plausible steel milling configuration, with 75% radial immersion. The chosen parameters are shown in the following table.

Parameter	Simbol	Value
No. of teeth	N	4
Entry angle	φ_{in}	0°
Exit angle	φ_{out}	120°
Spindle speed	Ω	600 rpm
Feed rate	s_t	0.2 $\frac{mm}{tooth}$
Tangential cutting coeff.	K_t	1800 $\frac{N}{mm^2}$
Radial cutting coeff.	K_r	0.33
Depth of cut	a	3-6 mm

Table 2.1: Cutting parameters

Looking at the depth of cut, the two different values are used to simulate both stable (3 mm) and unstable (6 mm) cutting conditions. In stable conditions, the two formulations bring to almost coincident results (Figures 2.5 and 2.6), because the difference relies on how the instability component is computed and in stable conditions it is almost negligible.

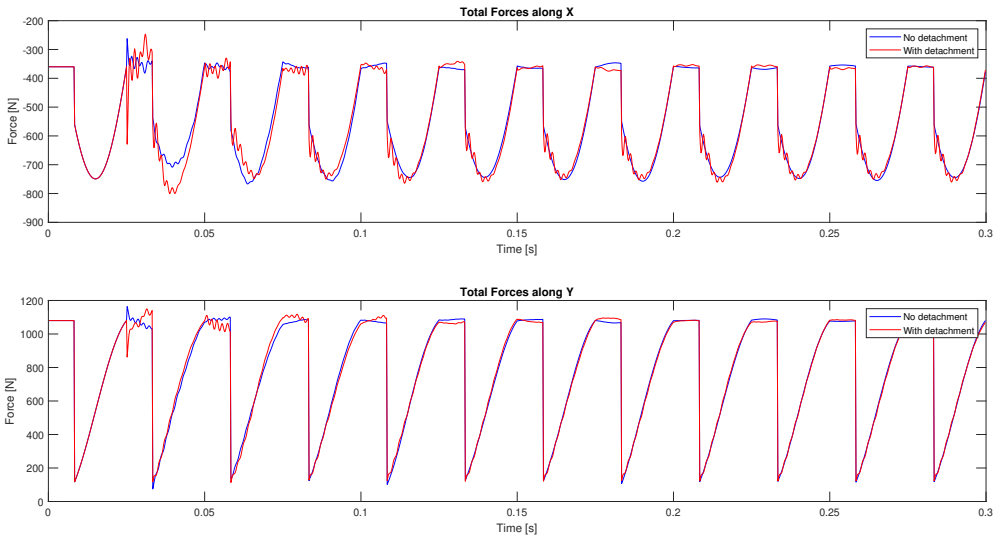

Figure 2.5: Total forces in stable conditions

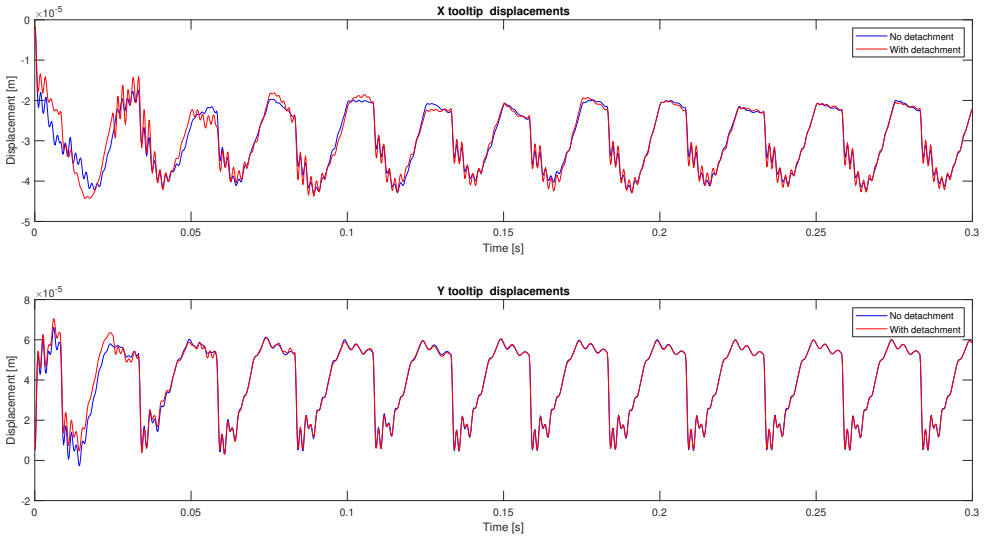

Figure 2.6: Tooltip displacements in stable conditions

The difference is considerable in unstable conditions, as it is possible to see in Figure 2.7 and Figure 2.8. The formulation with the detachment grows more rapidly in the first tooth passes, but it reaches a sort of pseudo-stationarity pretty soon thanks to the detachment. On the other hand, the Zero Order approach, since it does not include the detachment phenomenon, leads to an indefinite grow of forces and vibrations, which are soon higher and no longer reasonable.

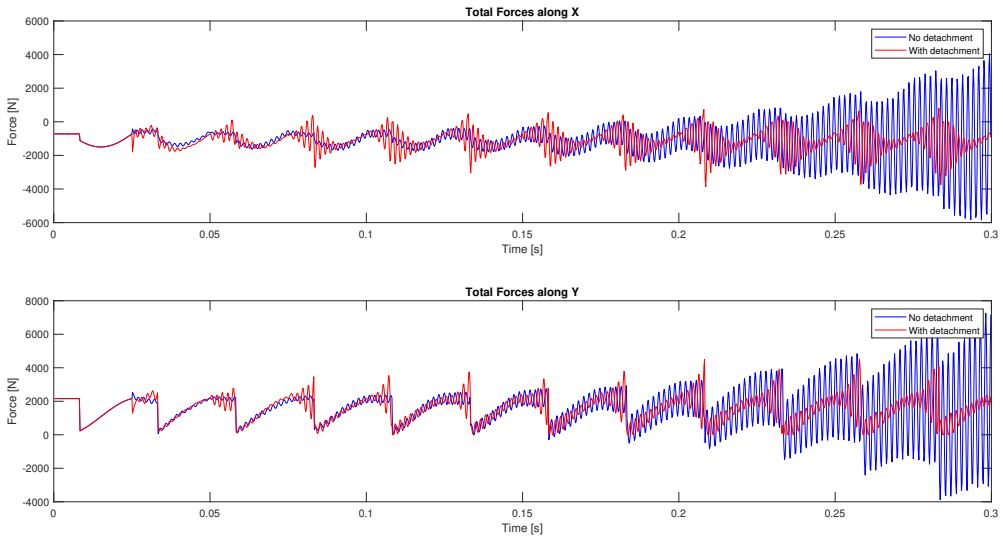

Figure 2.7: Total forces in unstable conditions

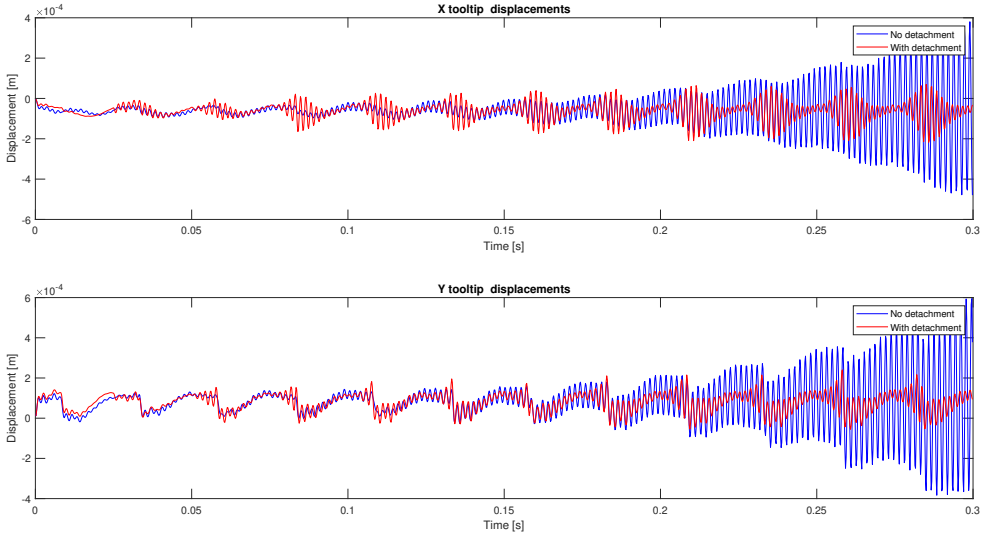

Figure 2.8: Tooltip displacements in unstable conditions

3 | Particle Filter design

3.1. Graphical abstract

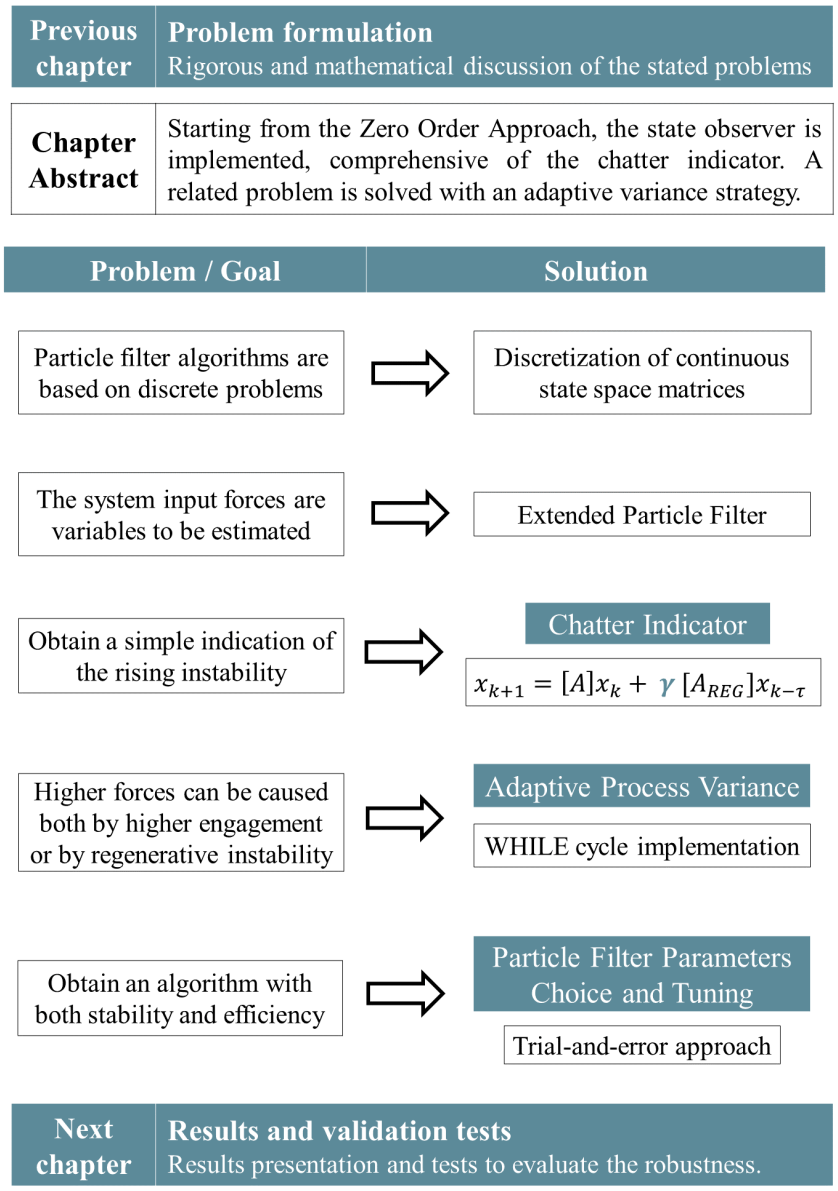

In this chapter, the development of the observer is analysed. It was chosen to show the implementation as it has been conceived, starting from more trivial concepts and then implementing consequential improvements.

As a starting point, the model described by Equation (2.14) is chosen as the process equation. It has a more compact form and it does not rely on the tooth angle at each time step, thanks to the averaging performed.

3.2. Formulation of discrete matrices

The first challenge was that the particle filter is conceived for discrete systems, while previous studies were all relying on continuous formulation. Jugo [6] offered an approximated strategy to obtain the corresponding discrete matrices starting from continuous ones. Thanks to his work, it was possible to switch from the continuous formulation of Equation (2.14) to the discrete form:

$$x_{k+1} = \mathbf{A_d} x_k + \mathbf{A_{d,REG}} x_{k-\kappa} + \mathbf{B_d} F_{NOM} \tag{3.1}$$

where $\kappa = \frac{\tau}{Ts}$ and Ts is the sampling time. In particular:

$$\mathbf{A_d} = e^{\mathbf{A}Ts} \tag{3.2a}$$

$$\mathbf{A_{d,REG}} = \mathbf{A^{-1}} \left(\mathbf{A_d} - \mathbf{I}\right) \mathbf{A_{REG}} \tag{3.2b}$$

$$\mathbf{B_d} = \mathbf{A^{-1}} \left(\mathbf{A_d} - \mathbf{I}\right) \mathbf{B} \tag{3.2c}$$

The second challenge is the creation of extended matrices, since the input force is not known, in order to obtain the following system:

$$\begin{Bmatrix} q_{k+1} \\ F_{k+1} \end{Bmatrix} = \begin{bmatrix} [Ad] & [Bd] \\ [0] & [I] \end{bmatrix} \begin{Bmatrix} q_k \\ F_k \end{Bmatrix} + \begin{bmatrix} [Ad_{REG}] & [0] \\ [0] & [0] \end{bmatrix} \begin{Bmatrix} q_{k-\kappa} \\ F_{k-\kappa} \end{Bmatrix} \tag{3.3a}$$

$$\begin{Bmatrix} y_k \end{Bmatrix} = \begin{bmatrix} [C] & [0] \end{bmatrix} \begin{Bmatrix} q_k \\ F_k \end{Bmatrix} \tag{3.3b}$$

In order to obtain this formulation, a strong assumption is made: the force is constant, in fact the force value at the step $k+1$ is coincident with the value at the step k. This uncertainty is compensated by the process variance.

It is now possible to focus on the actual particle filter algorithm, with the implementation of the process and measurement equations.

3.3. Process Equation

It can be observed in Algorithm 1.1 that at each time step, the distribution of the previous step is updated thanks to the *ProcessEquation*, exploiting the known mathematical model and introducing a stochastic process variance Q. The design of the process equation and the tuning of the aforementioned variance is one of the most delicate part of the whole process. For each of the N particles, the process equation starts with:

$$\begin{aligned} Fx_k &= Fx_{k-1} + Q * \mathcal{N}(0,1) \\ Fy_k &= Fy_{k-1} + Q * \mathcal{N}(0,1) \end{aligned} \tag{3.4}$$

These two new values are introduced in the state vector and the system is updated with Equation (3.3a), which is reported below in a more compact form.

$$\left\{ \begin{array}{c} q_{k+1} \\ F_{k+1} \end{array} \right\} = [A_d]^{ext} \left\{ \begin{array}{c} q_k \\ F_k \end{array} \right\} + [A_{d,REG}]^{ext} \left\{ \begin{array}{c} q_{k-\kappa} \\ F_{k-\kappa} \end{array} \right\} \tag{3.5}$$

The set of N state vectors represents the prior distribution. The next step is the calculation of the estimated measurements that each sample would be expected to create. This is performed with the $MeasurementEquation$, which was already shown in Equation (3.3b) and is reported below in a more compact form.

$$\left\{ y_k \right\} = [C]^{ext} \left\{ \begin{array}{c} q_k \\ F_k \end{array} \right\} \tag{3.6}$$

The estimated measurements are compared with the actual measurements coming from the sensors mounted on the spindle. A *weight* is assigned to each particle, calculated with the $LikelihoodFunction$from a multivariate distribution depending on the measurement variance matrix $[R]$. Particles which led to estimated measurements closer to the actual ones will obtain a higher weight, which means that, given the measurement, they are the most suitable to describe the evolution of the system at the specific time step. During the *resampling* stage, particles with higher weights are more likely to be saved and therefore to contribute at the identification of the posterior distribution of the state, whose average will be the saved as the final value for that time step.

3.4. Chatter indicator

After having fully understood the working principle of the shown process equation, it is possible to describe the focal point of this work: the implementation of a chatter indicator. The lone estimation of forces may not be enough for the complete comprehension of the cutting process. An increasing profile of forces and vibrations can be both a consequence of different tool engagement required by the part program and of the rising instability. The chatter indicator will help in the discrimination between these two possibilities.

The chatter indicator γ is thought as a state variable, whose value can be only 0 if the system is stable and 1 when it is unstable. The difference between the two configuration is $[A_{REG}]$, whose contribution is negligible in stable conditions but it is needed to describe the chatter phenomenon.

Therefore, the system is further extended, in order to include the chatter indicator as an additional state variable. Than, half of the population of N samples will be assigned $\gamma = 1$ while the other half will have $\gamma = 0$. After the stochastic estimation of forces described by Equation (3.4), which is not modified, the next step in the *ProcessEquation* is:

$$\begin{Bmatrix} q_{k+1} \\ F_{k+1} \\ \gamma_{k+1} \end{Bmatrix} = \begin{bmatrix} [Ad] & [Bd] & [0] \\ [0] & [I] & [0] \\ [0] & [0] & 1 \end{bmatrix} \begin{Bmatrix} q_k \\ F_k \\ \gamma_k \end{Bmatrix} + \boldsymbol{\gamma} \begin{bmatrix} [Ad_{REG}] & [0] & [0] \\ [0] & [0] & [0] \\ [0] & [0] & [0] \end{bmatrix} \begin{Bmatrix} q_{k-\kappa} \\ F_{k-\kappa} \\ \gamma_{k-\kappa} \end{Bmatrix} \tag{3.7}$$

The next part of the algorithm remains unchanged. Particles with the correct γ will be privileged in the resampling stage. After performing the average at the end of the time step, the value of the chatter indicator is expected to be close to 1 in unstable conditions and close to 0 in stable cutting. It will be shown in the following chapter that this prediction was not fully respected.

3.5. Adaptive process variance strategy

The implementation of the chatter indicator brings out a problem stated in the previous section. An increasing profile of forces and vibrations can be both a consequence of higher tool engagement or of the rising instability. The particle filter is still not able to detect this difference. Some particles may obtain good likelihoods thanks to $\gamma = 1$, other particles thanks to higher cutting forces. The tuning stage has not been treated yet, but it is possible to anticipate that the process variance value was set quite high ($Q \sim 1000N$), in order to absorb the big step of the force profile when the tooth exits from the material (Figure 2.5). A smaller process variance would improve chatter indicator performances,

but it also would lead to the failure of the algorithm when the angle of the first tooth φ_1 becomes higher than φ_{out}. An adaptive process variance cycle is implemented. The basic principle is to start from a small process variance, perform a step and calculate the residual weights. If the best weight is lower than a certain value, expressed as a percentage of the maximum achievable (estimated measurement coincident with the actual one), the process variance is increased and the time step repeated. In pseudocode:

Algorithm 3.1 Adaptive Variance

1: Set $c = 0$, $Q = Q_0$
2: **while** $c < pc_{max}$ and $Q < Q_{max}$ **do**
3: Update the system $x_{k+1}^- = ProcessEquation(x_k^+, Q)$
4: Estimate the measurements $y_{k+1}^- = MeasurementEquation(x_{k+1}^-)$
5: Calculate the residual weights
6: Set $c = max(ResidualWeights)$
7: Increase Process Variance $Q = nQ$
8: **end while**

where p is the aforementioned percentage of the maximum achievable likelihood, expressed as:

$$c_{max} = \frac{1}{4\pi^2\sqrt{|R|}} \tag{3.8}$$

n represents the speed at which Q is increased. It can be observed that the increase of the process variance is performed after the assignment of weights to each particle. In this way, the chatter indicator is privileged, and only if it is not enough to describe a force variation, the variance is updated.

3.6. Particle filter parameters choice

For the particle filter algorithm devised in this work, different parameters have to be set, in order to obtain a stable and efficient implementation.

First of all, all cutting parameters are needed for the writing of regenerative matrices. The more precise they are, the better performances will be. The covariance matrix is assembled with variance values obtained from a zero measure on both displacement and

acceleration sensors.

$$V = \begin{bmatrix} 3.6 \times 10^{-15} & 0 & 0 & 0 \\ 0 & 3.6 \times 10^{-16} & 0 & 0 \\ 0 & 0 & 0.01 & 0 \\ 0 & 0 & 0 & 0.01 \end{bmatrix} \tag{3.9}$$

The number of particles N should be kept as lower as possible for computational reasons. On the other hand, there is a minimum value, depending on the complexity of the system and on the number of states. Snyder [10] identifies a possible link between number of states N_s with the minimum number of particles required.

$$\log_{10} N = 0.05 N_s + 0.78 \tag{3.10}$$

It was obtained calculating the regression of some recursive tests that he performed. The obtained value should be $N \sim 10000$, but after some tests, it was decided to choose $N = 2000$ to keep computational time lower. This was probably possible because the process variance is concentrated in just three state variables (F_x, F_y and γ) and not spanned all over the 67 states. The other parameters are connected with the process variance and its adaptive cycle. There is not much literature about this tuning process, because it is too dependant on the particular process, so a trial-and-error strategy was adopted.

Parameter	**Value**	**Motivation**
Q_0	50 N	The maximum difference between two consecutive steps can be even lower, but thanks to the high number of particles the distribution is already well sampled.
p	20%	This value already represents a good match between true and estimated measurements. A higher value will cause the entrance in the while cycle also when not needed.
Q_{max}	1500 N	The principle of this choice was already explained: it depends on the maximum jump of forces which occur when the tooth exits the material
n	2	This parameter does not affect much the stability of the algorithm. It was chosen as a compromise between speed of computing and definition of the variance spectrum.

Table 3.1: Variance related parameters

4 | Results and validation tests

4.1. Graphical abstract

Previous chapter	**Particle filter design** Accurate description of the implemented algorithm
Chapter Abstract	Simulated results with both formulations are discussed. A comparison with previous models is done. Finally, results of estimation in real cutting conditions are shown.

Stable conditions → Good forces and vibrations estimations

Stable conditions → Chatter indicator $\gamma = 0.5$

Unstable conditions

Unstable conditions → Zero Order Approach

Unstable conditions → Tool Detachment

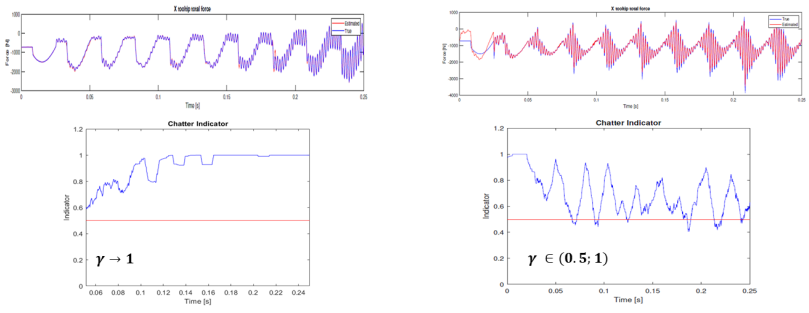

Off-design performances → In both nominal and off-design conditions, the particle filter outperforms the previous works

Experimental data → Good forces and vibrations estimation. The chatter indicator is not properly working.

Next chapter	**Conclusion and future works** Final considerations and possible improvements.

4.2. Simulation with Zero Order Approach

In this section, the plant is simulated with the Zero Order Approach, with the same cutting parameters shown in Section 2.6. In this condition, the particle filter should perform at its best, since the plant is simulated with the exact same model implemented in the observer. Both for stable and unstable conditions, plots regarding tooltip vibrations, cutting forces, process variance and chatter indicator will be shown.

4.2.1. Stable conditions

In stable conditions, the estimated tooltip vibrations (Figure 4.1) practically coincide with the actual ones. The resampling stage is working properly, the direct link between housing and tooltip measurements expressed by matrix $[C]$ is exploited at his best.

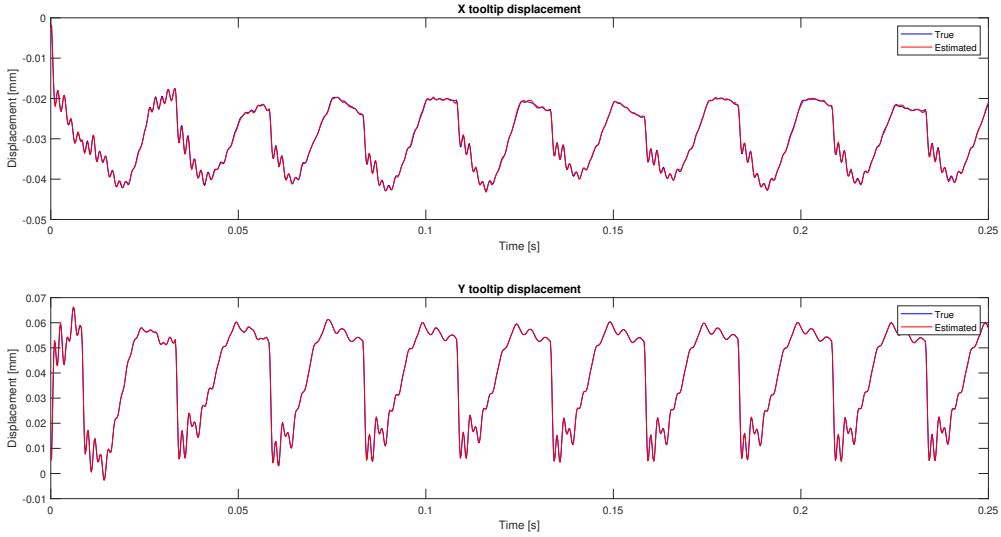

Figure 4.1: Tooltip displacements in stable conditions

As regards the forces, the profiles again almost coincide (Figure 4.2). The particle filter is able to absorbe in a few steps the big jumps of the forces, which are significant especially along Y direction.

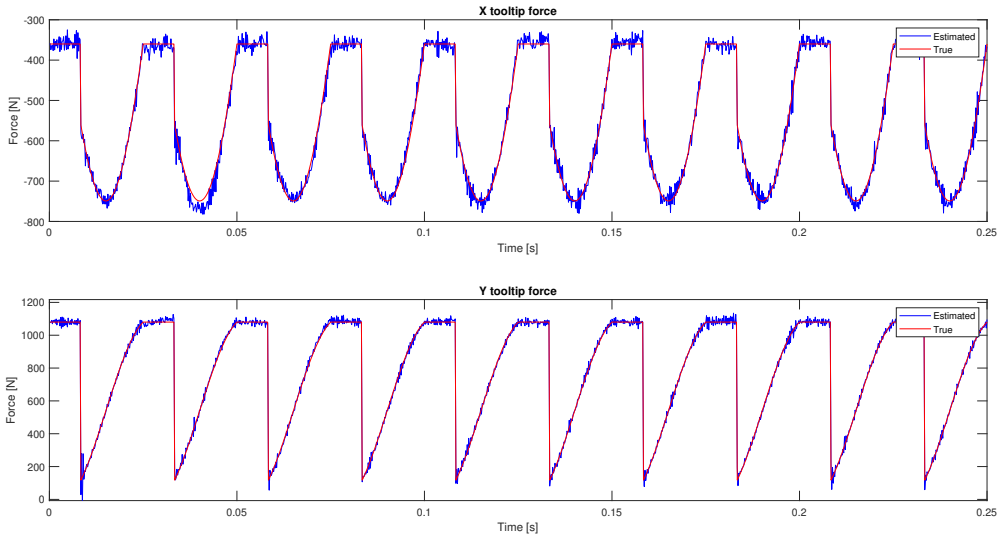

Figure 4.2: Cutting forces in stable conditions

The process variance (Figure 4.3) remains at its minimum for the most part of the simulation, except when the tooth exits the material. In that case, a higher value of variance is needed to follow the actual forces profile. The while-cycle is performing as it was thought during the design phase.

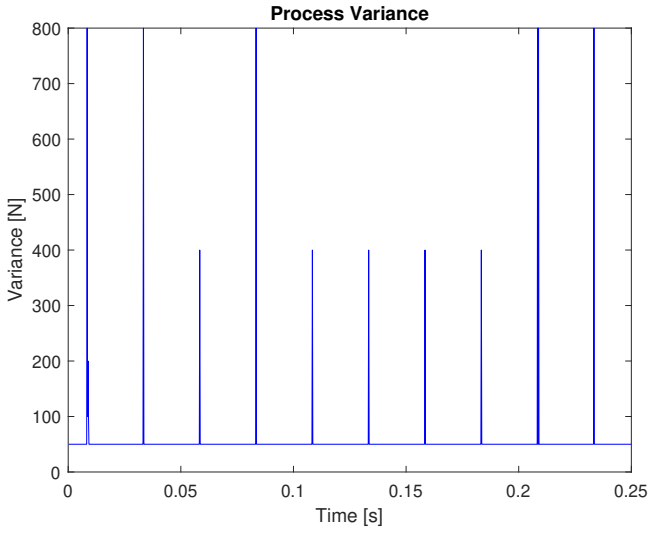

Figure 4.3: Adaptive process variance in stable conditions

As regards the chatter indicator plot (Figure 4.4), the first 0.03 seconds of the simulation represent the transient period in which the observer does not have any information of the previous tooth dynamics, since it is the first one approaching. After this small amount

of time, the chatter indicator stabilize around 0.5. Even if the idea was to have $\gamma = 0$ in stable conditions, it was possible to foresee this behaviour: in stable conditions the contribution of $[A_{REG}]$ is so small that its presence does not make important difference. because tooltip vibrations are in-phase with the machine dynamics and there is not chip modulation. Particles with both values of γ are resampled and the final value is the average between them.

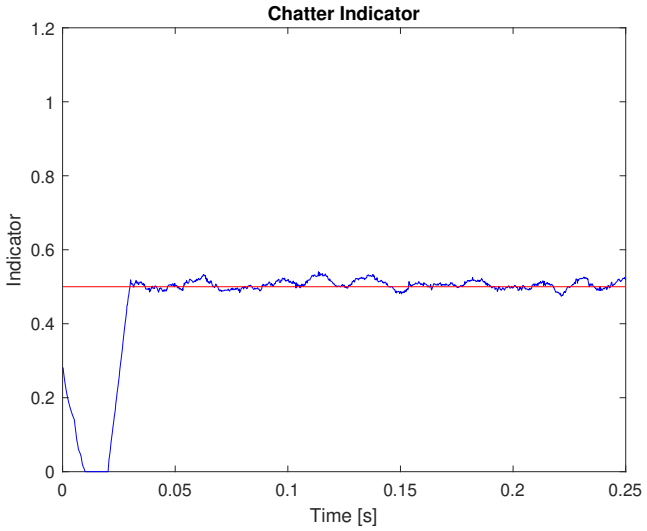

Figure 4.4: Chatter indicator in stable conditions

4.2.2. Unstable Conditions

The estimation of tooltip vibrations (Figure 4.5) in unstable conditions is as good as the stable ones, even if they are exponentially increasing foor the effect of the chip modulation.

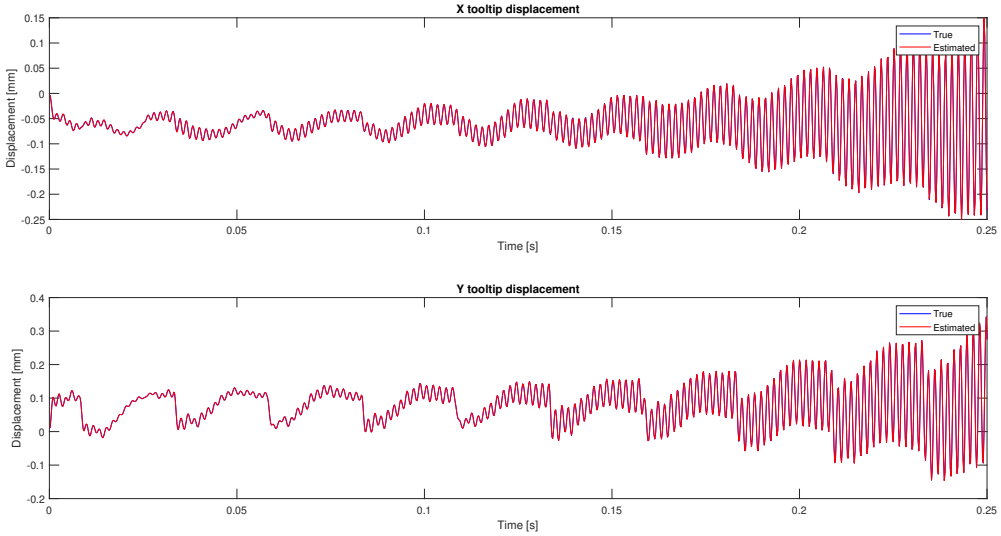

Figure 4.5: Tooltip displacements in unstable conditions

As regards the forces (Figure 4.6 and 4.7), it can be interesting to show separately the different contributions: nominal, regenerative and their sum. The estimation of the nominal force is as good as the one in stable conditions. The regenerative contribution, since it has a direct effect of vibrations, is also really good.

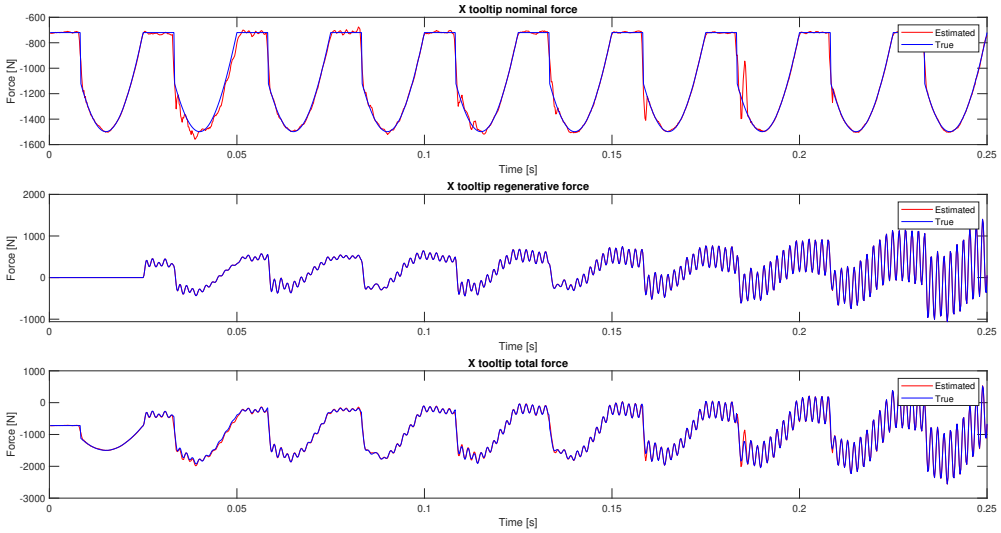

Figure 4.6: Cutting forces along X in unstable conditions

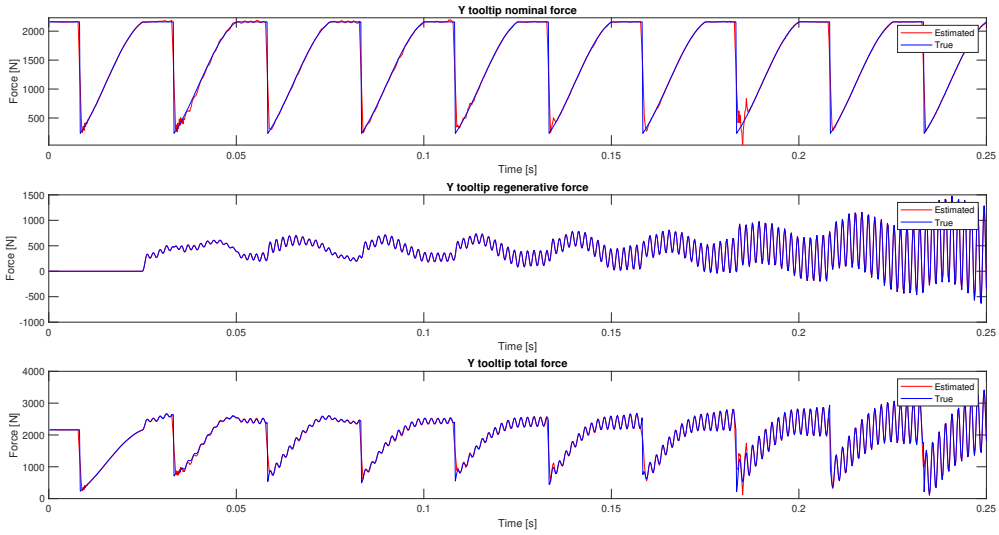

Figure 4.7: Cutting forces along Y in unstable conditions

The process variance (Figure 4.8) remains at its minimum for the most part of the simulation, except when the tooth exits the material. The behaviour is really similar to the stable conditions, but it can be observed that once the process variance is increased, it takes some additional step to go back to the minimum value, since the force is beginning to increasing as in stable conditions, but with a remaining strong oscillation at the chatter frequency.

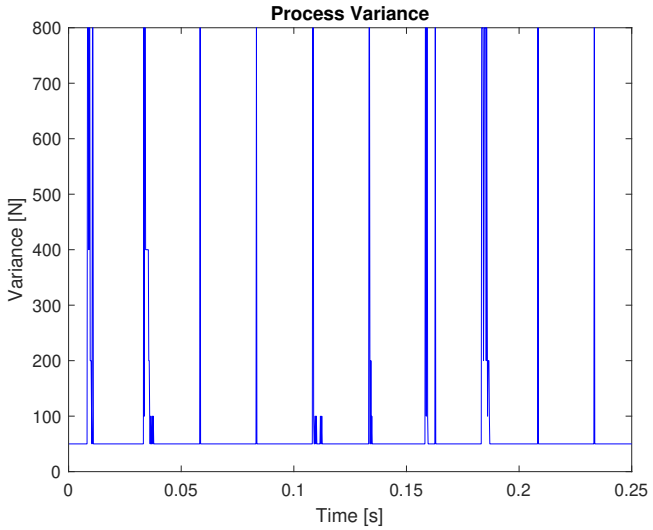

Figure 4.8: Adaptive process variance in unstable conditions

After the usual transient time, the chatter indicator (Figure 4.9) value begins to rise with

an oscillatory motion, whose frequency is the tooth passing frequency. In this period, the vibrations are high but they can still be justified with higher forces. After some tooth pass, the chatter indicator reaches and stabilizes above 0.95, meaning that the system is fully unstable and considering the regenerative contribution is mandatory for a good estimation.

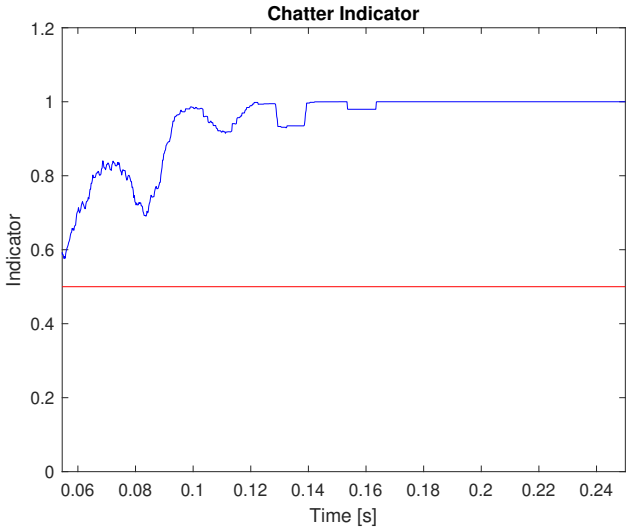

Figure 4.9: Chatter indicator in unstable conditions

4.3. Simulation with tool detachment

It was shown that in stable conditions, the two analysed formulations are really similar, because the regenerative contribution is really small. The results of the simulation with the detachment formulation are shown only for unstable conditions. The tooltip vibrations estimation is once again really good (Figure 4.10).

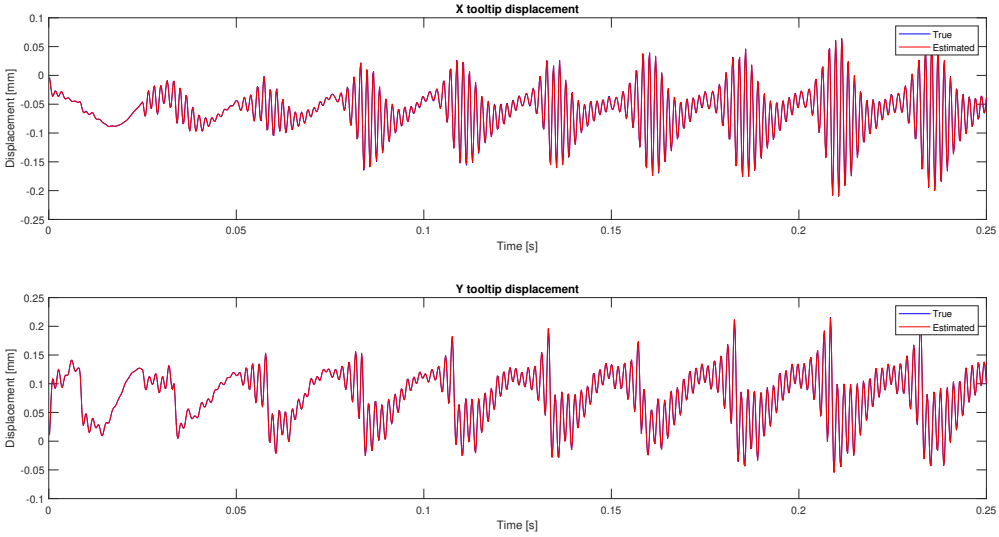

Figure 4.10: Tooltip displacements in unstable conditions

As regards the cutting forces (Figure 4.11), it is quite difficult to perform the separation between the nominal and the regenerative contribution, since the instability generated by the chip thickness modulation is alternatively absorbed by the nominal force and by regenerative vibrations. This behaviour will be easier to understand once the chatter indicator is shown. The total forces estimation is quite good, still some underestimation can be observed. This can be easily explained with the choice of implementing the observer with the Zero Order Approach, which is based on an averaging and it is more prone to loose picks in the force profile. The first 0.03 seconds of the plot, where profiles are different, can be explained with the missing information regarding the previous tooth pass, which are not available yet since the simulation has just started.

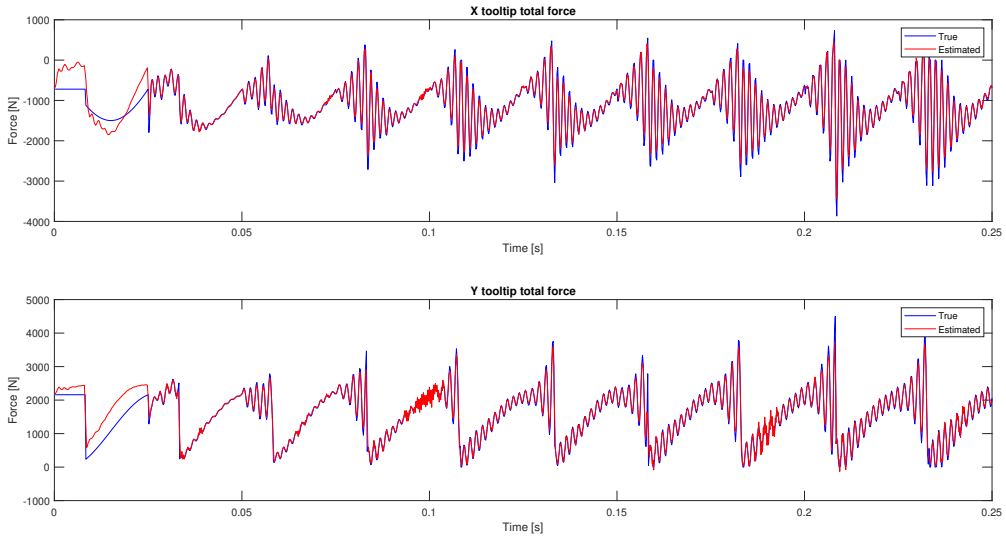

Figure 4.11: Cutting forces in unstable conditions

The process variance (Figure 4.12)is of course higher, the plant is simulated with a different formulation from the observer and the algorithm may need an increased variance to match measurements.

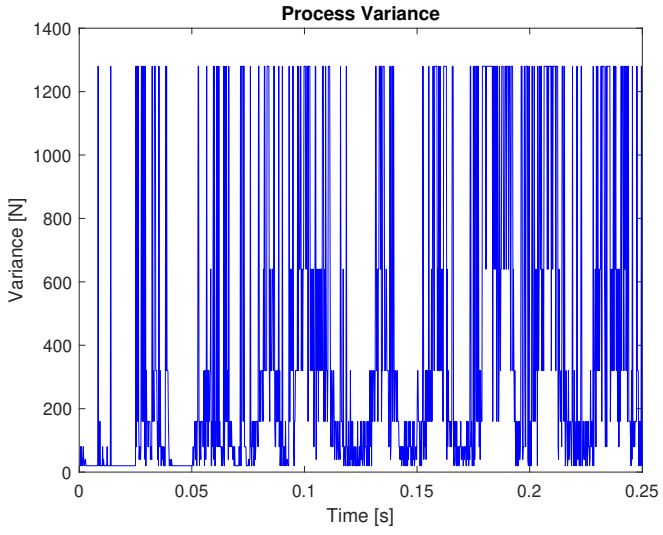

Figure 4.12: Adaptive Process Variance in unstable conditions

The chatter indicator (Figure 4.13) shows its best performances in this case. The detachment phenomenon is complex to be described because the instability is not irreversible: once the tool detaches from the workpiece, the system begins its ramp back from a stable condition. The chatter indicator fully describes this behaviour: it starts from 0.5, which is

the obtained value in stable conditions, it increases almost to 1 and then the detachment occurs. The particular tooth is not engaged and it is not able to contribute in the regenerative effect. So the chatter indicator falls back to the initial 0.5 when the tooth starts cutting again. This phenomenon is of course cyclical and the frequency of this oscillation is the tooth passing frequency.

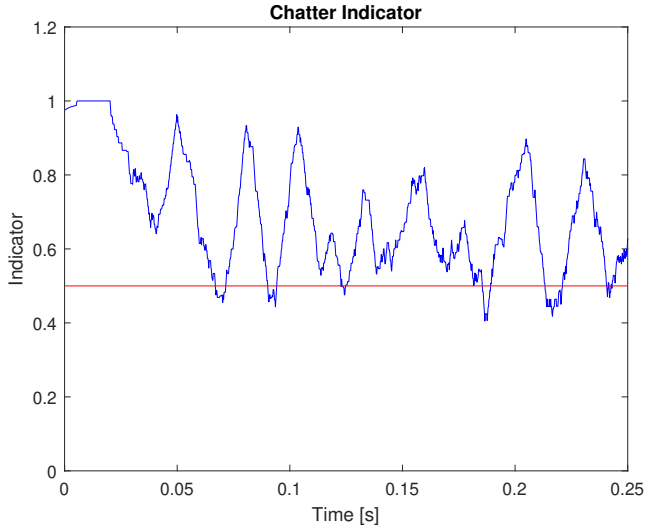

Figure 4.13: Chatter indicator in unstable conditions

4.4. Nominal performances and robustness analysis

The discussion about the results was only qualitative until this point. In this section, the performances will be analyzed from the point of view of the root mean square of the difference between the estimated values and the ones of the plant simulation. The particle filter will be compared with State of the Art methods in both nominal conditions and off-design conditions, which means that the parameters of the observer are set slightly different from the plant ones. This simulation is closer to experimental conditions, when information on the engagement or on the cutting coefficients may not be precise. In particular, the parameters which were modified were φ_{ex} and the element aK_t, considered as a product since they can be identified as the gain of the matrix $[A_{REG}]$.

Parameter	Plant	Observer (Nominal)	Observer (Higher engagement)	Observer (Lower engagement)
φ_{ex}	120°	120°	132°	108°
a	6 mm	6 mm	6.48 mm	5.7 mm

Table 4.1: Differences in parameters setting

These results are obtained in unstable conditions, since it does not make sense to verify performance in stable conditions when $[A_{REG}]$ is not affecting the observer performances. In nominal conditions, the parameters of the observer and of the plant simulation are coincident. Using the Zero Order approach the delayed observer [9] keeps better performances along Y-axis, while the particle filter is working much better along Y-axis.

Observer	Fx [N]	Fy [N]	Xtp [mm]	Ytp [mm]
Particle Filter	0.092	0.176	5.2e-7	2.2e-7
Delayed Observer	0.052	0.936	2.0e-9	3.1e-5

Table 4.2: Nominal conditions, Particle Filter vs Delayed Observer

When the plant is simulated with the tool detachment, the RMS of the error of the considered variables similar along X but much lower than the Kalman filter [11] along Y.

Observer	Fx [N]	Fy [N]	Xtp [mm]	Ytp [mm]
Particle Filter	0.694	0.76	1.0e-6	4.4e-7
Kalman Filter	0.49	2.39	1.2e-6	8.4e-5

Table 4.3: Nominal conditions, Particle Filter vs Kalman Filter

The Kalman filter does not require cutting parameters, so it is not possible to talk about off-design performances. This check is possible only for the comparison between the delayed observer and the particle filter, with the Zero Order approach in the plant simulation.

At first, the observer is set with a supposed higher engagement: the term aK_t is increased by 8% and φ_{ex} by 10%.

Observer	Fx [N]	Fy [N]	Xtp [mm]	Ytp [mm]
Particle Filter	0.196	0.32	6.8e-7	2.8e-7
Delayed Observer	0.45	1.46	2.8e-9	3.6e-5

Table 4.4: Higher engagement, Particle Filter vs Delayed Observer

Then, the observer is set with a supposed lower engagement: the term aK_t is reduced by 5% and φ_{ex} by 10%.

Observer	Fx [N]	Fy [N]	Xtp [mm]	Ytp [mm]
Particle Filter	0.134	0.246	7.0e-7	2.4e-7
Delayed Observer	0.458	1.24	2.2e-9	3.4e-5

Table 4.5: Lower engagement, Particle Filter vs Delayed Observer

In both these conditions, the only variable in which the delayed observer performs better is the estimation of tooltip vibrations along Y, thanks to the coincidence of the observer model with the simulated one. The real strong point of the particle filter is the cutting forces estimation, goal of this thesis, especially in non-ideal conditions. Thanks to its numerical formulation and the possibility to adapt the process variance in the most critical steps, it is able to absorb settings errors and to overcome differences in the formulations.

4.5. Possibility of degeneration of the algorithm

It is a known problem for particle filters [7] that in some case the algorithm can resample only one particle, because there is only one sample with a likelihood different from zero. In order to verify that this problem does not occur, a plot of the whole particles population is shown.

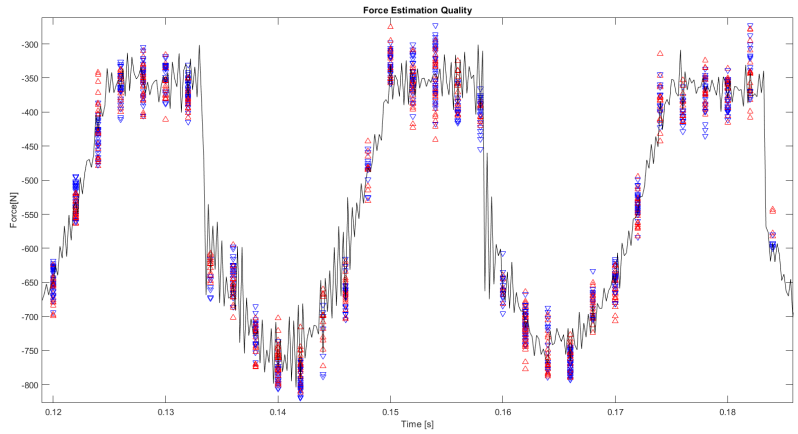

Figure 4.14: Particle population in stable conditions

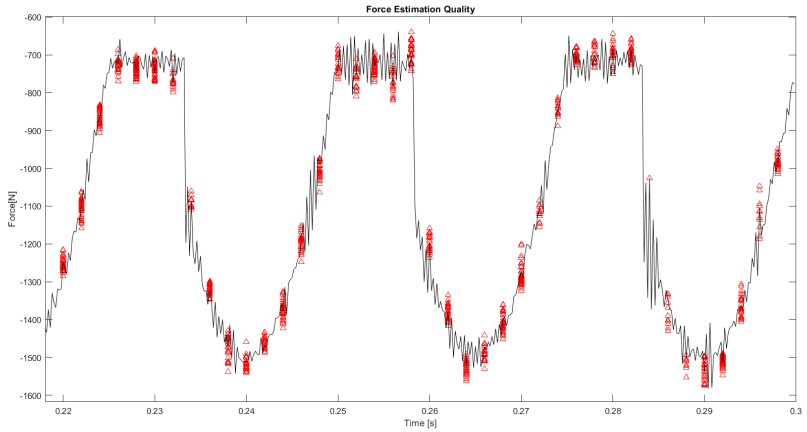

Figure 4.15: Particle population in unstable conditions

It can be observed that in both situations, a good number of particles is resampled at each step. In particular, blue triangles represent stable samples ($\gamma = 0$), while red triangles represent unstable particles ($\gamma = 1$). In stable conditions, there is almost the same amount of red and blue triangles, for the already explained reason of small regenerative contribution. In unstable conditions, the amount of resampled particles is once again a good number, but there are only red triangles, because only unstable particles are resampled.

4.6. Experimental Data

Finally, the most challenging section is the test of the particle filter algorithm in real cutting conditions. The sensors configuration used during the cutting tests is shown in Figure 4.16 and includes inductive relative displacements sensors on the tooltip, tri-axial spindle housing accelerometers and inductive relative displacements sensors on the spindle housing.

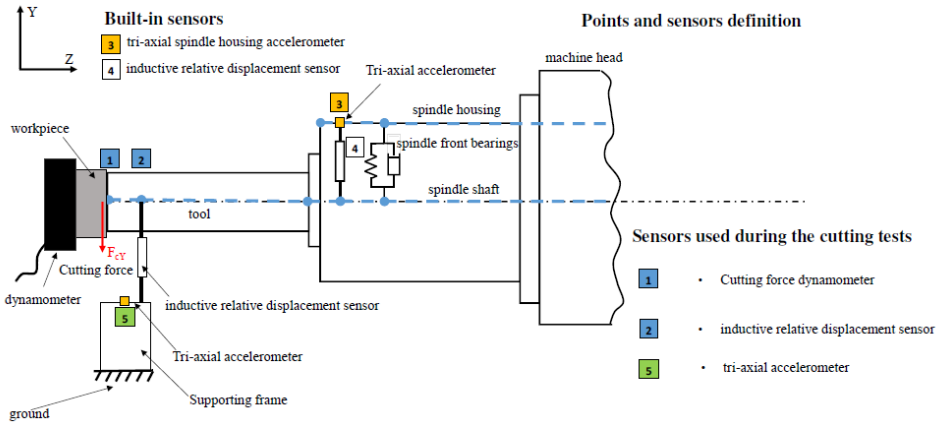

Figure 4.16: Sensors for cutting tests

The cutting parameters are slightly different from the simulation ones. The simulation goal was to show a periodic tooth engagement, while in cutting experiments it is common practice to perform slot milling.

Parameter	Simbol	Value
No. of teeth	N	4
Entry angle	φ_{in}	0°
Exit angle	φ_{out}	180°
Spindle speed	Ω	915 rpm
Feed rate	s_t	0.2 $\frac{mm}{tooth}$
Tangential cutting coeff.	K_t	1800 $\frac{N}{mm^2}$
Radial cutting coeff.	K_r	0.33
Depth of cut	a	3.5-4.5 mm

Table 4.6: Cutting parameters

4.6.1. Stable cut

In stable conditions, it is possible to see that tooltip vibrations (Figure 4.17) and cutting forces (Figure 4.18) are estimated quite well, even if some differences are caused by the introduction of the dynamometer dynamics. Of course it is difficult to obtain results as good as the simulations, because many approximations and simplifications are made in the modelization of the problem.

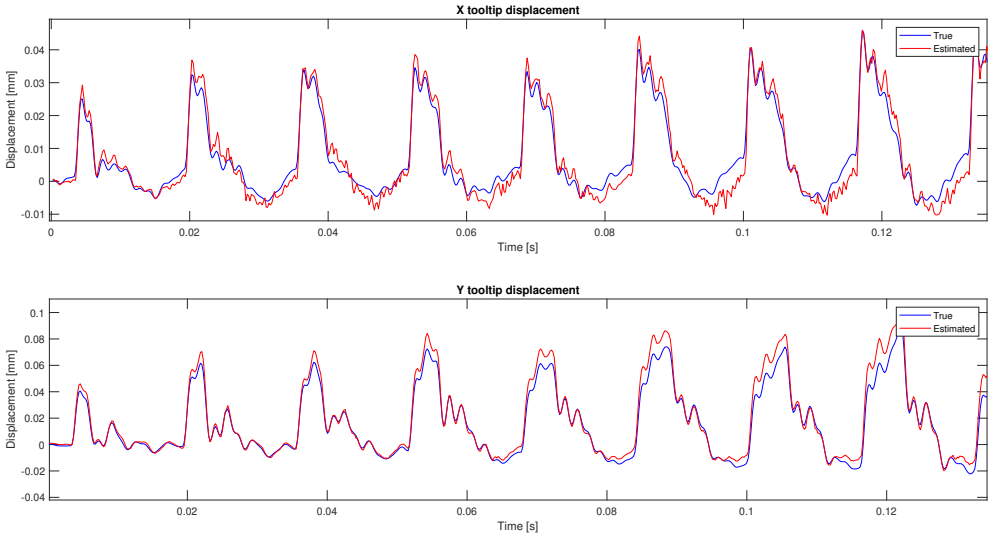

Figure 4.17: Tooltip displacements in stable conditions

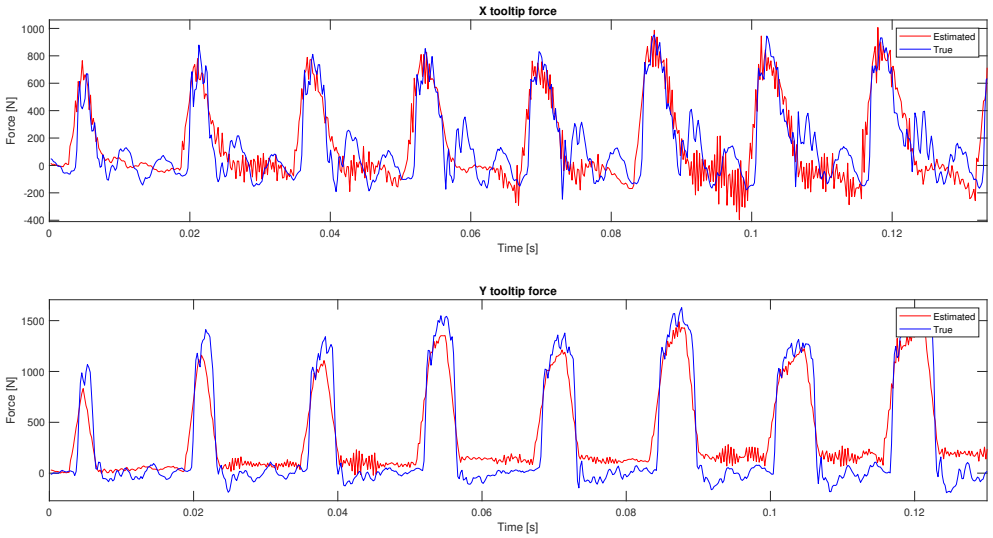

Figure 4.18: Cutting forces in stable conditions

The process variance (Figure 4.19) is generally higher, because the theoretical system implemented in the observer is only an approximation of the machine.

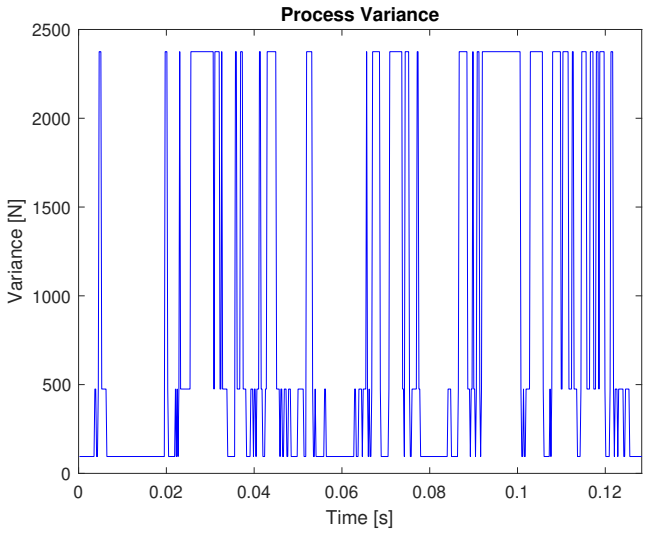

Figure 4.19: Adaptive process variance in stable conditions

As regards the chatter indicator (Figure 4.20), the average is as expected close to 0.5. Of course it is possible to see some larger oscillation around this value, but generally speaking it is a good result.

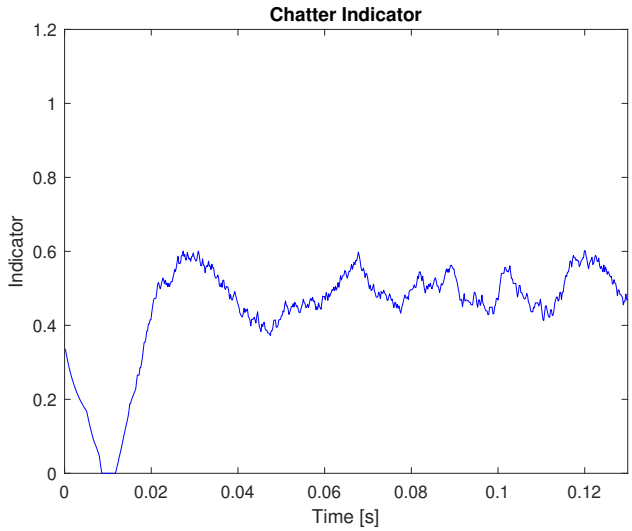

Figure 4.20: Chatter indicator in stable conditions

4.6.2. Unstable cut

In unstable conditions, the performances does not change much. The experiment is performed in slightly unstable conditions (the axial depth of cut is 4.5 mm while in the simulation it was 6 mm) and the differences are not so evident (Figure 4.21 and 4.22).

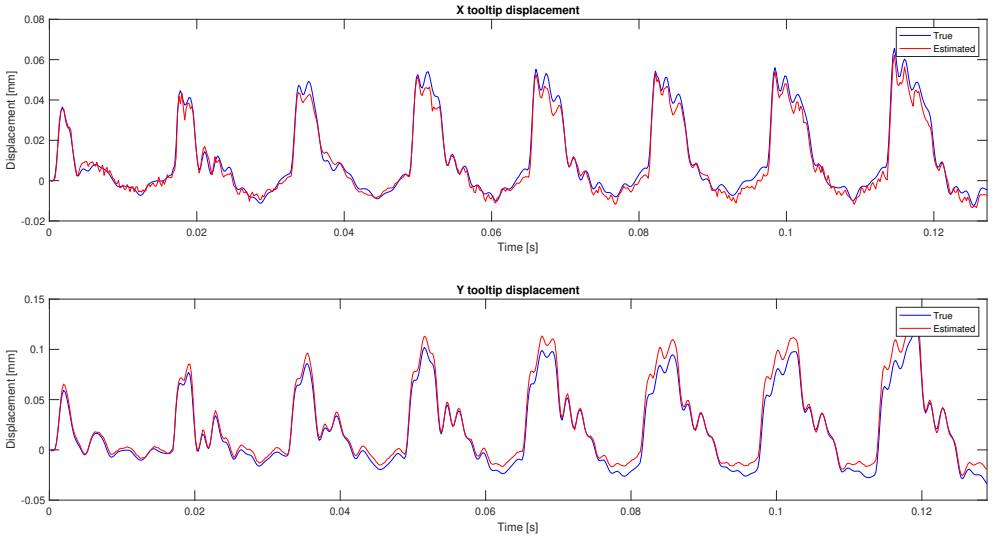

Figure 4.21: Tooltip displacements in unstable conditions

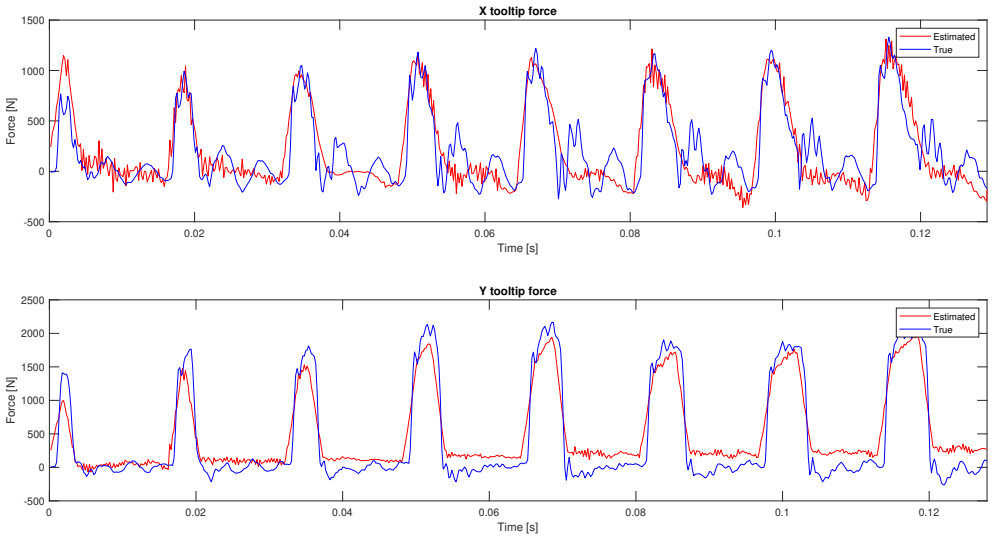

Figure 4.22: Cutting forces in unstable conditions

The process variance (Figure 4.23) can be a little bit higher than the one observed in

stable conditions, but once again the difference is not really high.

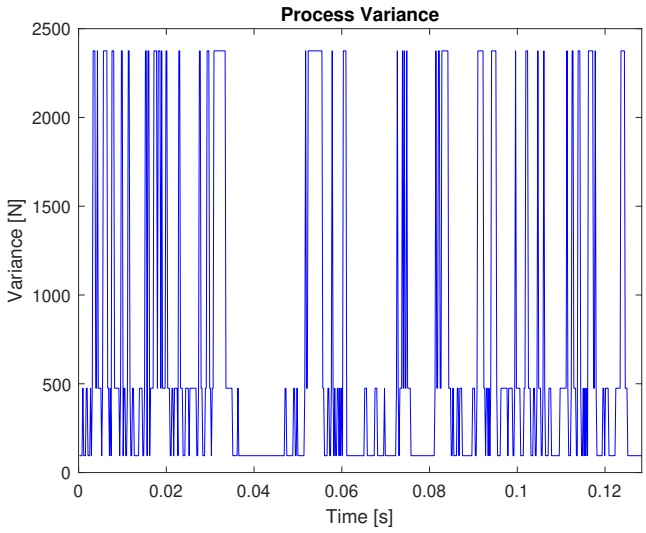

Figure 4.23: Adaptive process variance in unstable conditions

The chatter indicator (Figure 4.24) is not showing the expected behaviour. It can be seen that the average value is around 0.5 or slightly above and it is not possible to see an increasing trend, even if the experiment is performed in unstable conditions. This behaviour can be explained as a limit of the Zero Order approach. In fact, in the simulation environment, an axial depth of 4.5 mm is not enough to create chatter. The computed $[A_{REG}]$ may be not enough to bring the system of the observer to instability, but the particle filter algorithm is able to match the experimental measurements with a simple increase of forces. The presence of the regenerative contribution is not fundamental and the average value of the chatter indicator is 0.5.

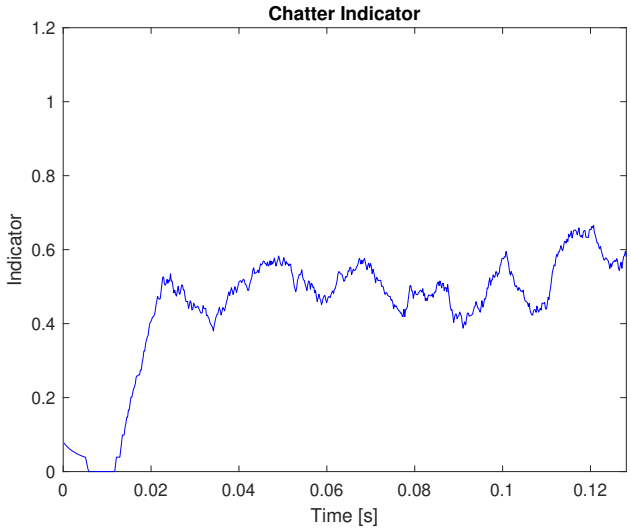

Figure 4.24: Chatter indicator in unstable conditions

5 | Conclusions and future developments

In this work, a state observer for the estimation of cutting forces and the detection of regenerative instability in milling exploting information from both the machine and the cutting process was implemented.

The work started with the study of the regenerative instability and with the identification of the possible challenges in cutting forces measurements, both direct and indirect, regarding the differences for the introduction of a dynamometer or for the development of a strong model model explaining the relationship between the force magnitude and the instrument reading. Previous methods for the estimation of forces and vibration in machining were analyzed and possible area of improvements were found. A review on the standard algorithm of a particle filter was provided, as the method able to merge already existent observers and improve them.

Milling is a complex process, which can be formulated with different levels of approximation. The plant was simulated considering the Zero Order approach at first, and then introducing the tool detachment. The observer is designed based on the Zero Order approach formulation, more suitable to be introduced in the process equation. It required the discretization and the extension of the state space matrices, in order to include forces as state variables. The implementation of the chatter indicator was only a consequence of the high customizability of the particle filter, even if it required some modification in the algorithm and a delicate parameters tuning.

In the simulation phase, the conceived observer performed as expected or even better. The chatter indicator resulted to be a robust parameter which offered interesting considerations. The estimation in real cutting conditions proved to be an important starting point as regards forces and tooltip vibrations, even if the correct functioning of the chatter indicator was not achieved.

Future works may take two different directions. The first one is the optimization of the current algorithm, in order to reduce the computational cost of one single time step.

Number of internal states, number of particles or sampling frequency are still high, but they are needed for a correct working of the algorithm. A reduction of them may result in the feasibility of an online observer, in which the cycle time is lower than the sampling time. The other direction is the introduction of the cutting parameters as unknown variables, since the workpiece fixing may be not optimal. This modification can improve performances in real cutting conditions, where cutting coefficients or parameters may not be so precise. On the other hand, increasing the number of states is in clear disagreement with the goal of problem simplification, needed for an online observer.

Bibliography

[1] P. Albertelli, M. Goletta, M. Torta, M. Salehi, and M. Monno. Model-based broadband estimation of cutting forces and tool vibration in milling through in-process indirect multiple-sensors measurements. *International Journal, Advanced Manuf. Technol.*, 2004.

[2] A. Albrecht and Y. Park, S.and Altintas. High frequency bandwidth cutting force measurement in milling using capacitance displacement sensors. *International Journal of Machine Tools and Manufacture*, 2005.

[3] Y. Altintas and E. Budak. Analytical prediction of stability lobes in milling. *CIRP Ann. - Manuf. Technol.*, 1995.

[4] Y. Altintas and S. S. Park. Dynamic compensation of spindle-integrated force sensors. *J. Dyn. Syst. Meas. Control*, 2004.

[5] J. Hol. Resampling in particle filters. Master's thesis, Linkoping University, 2004.

[6] J. Jugo. Discretization of continuous time-delay systems. *Elsevier IFAC Publications*, 2002.

[7] R. Karlsson. *Partile filtering for positioning and tracking applications*. PhD thesis, Linkoping University, 2005.

[8] Z. Li and Q. Liu. Solution and analysis of chatter stability for end milling in the time-domain. *Chinese Journal of Aeronautics*, 2008.

[9] D. Marzatico. State estimation for delayed systems.an innovative application for cutting force estimation in face milling with regenerative chatter instability. Master's thesis, Politecnico di Milano, 2018.

[10] C. Snyder, T. Bengtsson, P. Bickel, and J. Anderson. Obstacles to high-dimensional particle filtering. *American Meteorological Society*, 2008.

[11] G. Torricella. Estimation of cutting forces and tool tip vibrations in milling in stable and unstable conditions. Master's thesis, Politecnico di Milano, 2019.

[12] G. Welch and G. Bishop. An introduction to the kalman filter. *University of North Carolina at Chapel Hill*, 1997.

List of Figures

List of Tables

Acknowledgements

Vorrei dedicare questo spazio a tutte le persone che hanno contribuito al raggiungimento di questo obiettivo.

Per iniziare, un ringraziamento al mio relatore, Prof. Paolo Albertelli, per la disponibilità e le conoscenze trasmessemi con passione. Grazie all'Ing. Luca Bernini, che mi ha seguito quasi settimanalmente con costanza e competenza nella stesura di questo elaborato.

Vorrei ringraziare tutte le persone che ho incontrato nel mio percorso universitario, in particolare Federico, Filippo e Italo, conosciuti come colleghi ma diventati riferimenti importanti, con cui ho condiviso sì momenti difficili, ma soprattuto di amicizia, divertimento e crescita personale.

Un grazie enorme agli amici di una vita, Bocia, Bomba, Gone, Nick e Teino, certezze su cui ho sempre potuto contare.

Grazie alla mia fidanzata Sara, che era già al mio fianco il giorno in cui ho iniziato questo capitolo della mia vita ed è qui ora, dopo avermi compreso in ogni sessione d'esame, appoggiato in ogni scelta e supportato con prezioso affetto in ogni momento di questi cinque anni.

Grazie a mia nonna Albina e a mio zio Andrea, per quello che rappresentano per me. Grazie a mia sorella Linda, che mi ha fatto sentire stimato in ogni momento e mi ha richiamato allo studio quando mi ha visto distratto.

E per finire, il ringraziamento più grande ai miei genitori, Davide e Simona, per il supporto incondizionato che mi hanno dato, per i sacrifici fatti per garantirmi le migliori possibilità senza farmeli pesare nemmeno per un istante. Per avermi ispirato, per avermi spronato quando ne necessitavo e per aver intavolato il miglior futuro che un figlio possa desiderare.